



Final report

Biophysical Characterization of Riboflavin-Functionalized Superparamagnetic Iron Oxide Nanoparticles (Rf-SPIONs) for Riboflavin Carrier Protein Detection

Ву

Kanlaya Prapainop

November 2018

Contract No. MRG5980041

Final Report

Biophysical Characterization of Riboflavin-Functionalized Superparamagnetic Iron Oxide Nanoparticles (Rf-SPIONs) for Riboflavin Carrier Protein Detection

Kanlaya Prapainop

Mahidol University

Project Granted by the Thailand Research Fund and Office of the Higher Education Commission

Abstract

Project Code: MRG5980041

Project Title: Biophysical Characterization of Riboflavin-Functionalized Superparamagnetic

Iron Oxide Nanoparticles (Rf-SPIONs) for Riboflavin Carrier Protein Detection

Investigator: Kanlaya Prapainop

Mahidol University

E-mail Address: kanlaya.pra@mahidol.edu

Project Period: 2 years

Abstract:

Riboflavin carrier protein (RCP) has been shown recently as an alternative biomarker for cancer diagnosis. Because RCP level in serum has been found to be elevated in breast cancer, prostate cancer and hepatocellular carcinoma patients comparing to healthy groups. The conventional method for RCP detection is using radioimmuno assay (RIA) which involves radioactive compounds so it is considered to be unsafe and require license for performing the assay. In this research, an alternative method will be developed which is safer, easier and could be more sensitive comparing to the RIA technique. This new approach will be using superparamagnetic iron oxide nanoparticles (SPIONs) which have a great potential in nanomedicine due to the unique properties such as superparamagnetic behavior, stability, biocompatibility and ease of fabrication and surface engineering. Various synthesis conditions for SPIONs will be performed to achieve different sizes and different surface coatings of the NPs. After that the nanoparticles will be further conjugated with different amount of riboflavin (Rf) which is a ligand for RCP to achieve riboflavin functionalized SPIONs (Rf-SPIONs). In order to evaluate which synthesis condition give the best candidate for RCP binding, thermodynamic parameters between the Rf-SPIONs and RCP will be investigated using Isothermal Titration Calorimetry (ITC) and Differential Scanning Calorimetry (DSC) methods. Results of biophysical interaction studies will provide an important information of the role of sizes, surface coatings and quantities of surface ligands to the RCP binding. Fundamental knowledge on the interactions between Rf-SPIONs and RCP will elaborate the effective process of SPIONs synthesis design. This development can be applied to accurate cancer detection at early stage worldwide.

Keywords: Magnetic nanoparticles, riboflavin, binding affinity, Isothermal Titration Calorimetry, Differential Scanning Calorimetry

1. Executive summary

1.1 Introduction to research

Nanomedicine is the field that uses nanomaterials in medical research area for diagnosis, drug delivery or therapy. The materials for preparing nanoparticles can be organic or inorganic such as iron oxide, carbon, silica, silver, gold etc. The nanoparticles (NPs) can be further conjugated to biomolecules such as peptides, antibodies or nucleic acids and can be used as probes to follow cellular movements and molecular changes associated with pathological symptoms and for the detection and diagnosis of diseases in early states, especially in cancer research field¹ (figure 1a). One of the most widely studied research area is magnetic nanoparticles that have gained extensive attention because of their unique properties including superparamagnetic behaviour (figure 1b), stability, biocompatibility and ease of surface chemistry modification. The nanoparticle surface can be modified with specific ligand that can capture interested proteins. With the magnetism property, it then can be easily isolated/purified from complex biological environment that contains large amount of proteins and other biological molecules by applying the magnetic field. This method therefore can be used as a quick and efficient method for bio-separation application which is very useful for biotechnology and can be applied into medical applications such as in cancer research area.

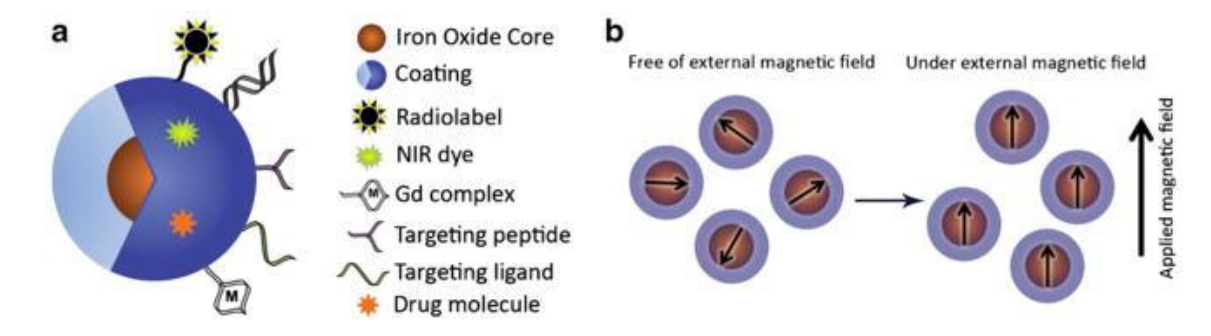


Figure 1. The magnetic nanoparticles. (a) The magnetic nanoparticle is composed of magnetic core and the coating with different moieties for additional functionalities. (b) Superparamagnetic iron oxide nanoparticles have a single magnetic domain because of their small magnetic core and are greatly magnetized under an externally applied magnetic field¹.

In cancer therapy, early detection is the best chance for successful and high survival rate. The most recent study has shown that riboflavin carrier proteins (RCP) in serum are elevated in cancer patients²⁻⁴. Therefore, RCP has potential to be used as a biomarker for early cancer detection. This research will be involved in developing magnetic nanoparticles decorated with riboflavin which is the RCP ligand in highly specific manner in order to be further used for an easy and simple technique for cancer diagnostic tool. The structure of riboflavin is shown in the figure 2. It is a component of FAD and FMN which plays important role in cellular metabolism, cell growth and development which is linked to cancer metabolism.

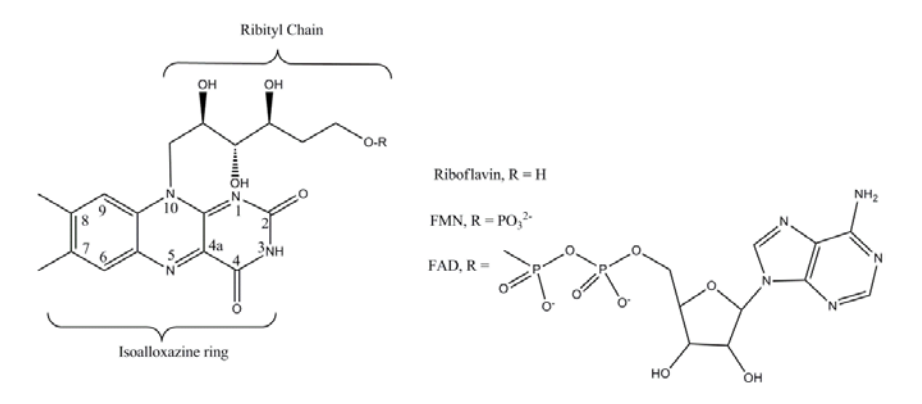


Figure 2. Structures of Riboflavin, FMN, and FAD.

The superparamagnetic iron oxide nanoparticles (SPION) amino-functionalized with riboflavin analog will be prepared as shown in the overall scheme below (figure 3). The riboflavin will serve as a targeting ligand on the surface of nanoparticles to bind to riboflavin carrier protein. The conditions to prepare the desired size of nanoparticles, the amount of ligands on the surface will be optimized for the best binding to RCP. The future development of the cancer detection could be performed directly from patient serum, however, with the magnetic nanoparticles, the isolating interested protein could also be obtained. This development of the nanoparticles that specifically target to riboflavin carrier protein will be another essential step to improve the early diagnostic of breast cancer which will increase the survival rate of patients. The future development could be used in combination with the chemiluminescence enzyme immunoassay (CLEIA) for detection of RCP serum.

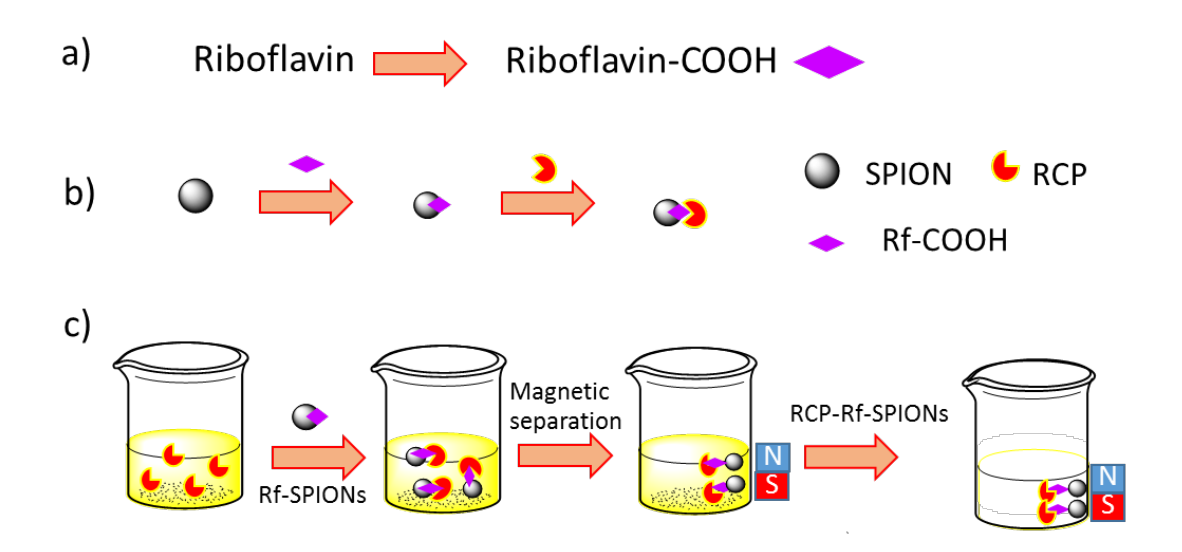


Figure 3. Scheme of superparamagnetic iron oxide nanoparticles (SPIONs) functionalized with riboflavin (Rf-SPIONs) for riboflavin carrier protein detection. A) Riboflavin analog is prepared for further conjugation on the SPIONs surface. B) SPIONs are functionalized with a riboflavin analog (Rf-COOH) that gives the best binding to riboflavin carrier protein (RCP). C) The SPIONs will be investigated the binding efficiency to RCP in the presence of other proteins.

1.2 Literature review

Magnetic nanoparticles (MNPs) have gained lots of interest in the past decades due to their unique properties such as superparamagnetism, high magnetic susceptibility and biocompatibility resulting in a wide range of research applications including catalysis⁵, biotechnology⁶, biomedicine⁷, and environmental remediation⁸. The superparamagnetic feature means that the nanoparticles are magnetized when applying magnetic field however, they lose the magnetic property after removing the magnetic field. This property allows us to be able to control the particle properties. For example, we can use the magnetic field when separation is needed and remove the magnetic field when the particles are required to be dispersed in the medium (figure 4). It can also be controlled the location of the deposit magnetic nanoparticles using magnetic field⁹. The magnetic nanoparticles can be synthesized by different methods such as co-precipitation, thermal decomposition, laser pyrolysis, micro-emulsion or hydrothermal synthesis. The co-precipitation method is the most facile, reproducible and convenient approach to synthesize iron oxide from aqueous Fe²⁺/Fe³⁺ salt solution by addition base under inert atmosphere at room temperature or higher temperature¹⁰. The

superparamagnetic iron oxide nanoparticles (SPIONs) are nanoparticles with a synthetic γ -Fe₂O₃ (magnetite), Fe₃O₄ (magnetite) or the combination of two.

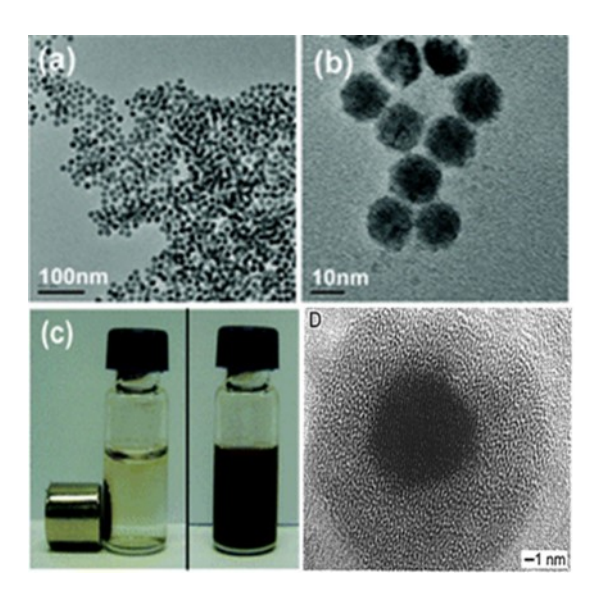


Figure 4. Magnetic nanoparticles. (a and b) TEM images of Ni magnetic nanoparticles. (c) Ni-MNPs with and without applying magnet¹¹. (d) TEM image of Iron oxide nanoparticles with silica surface coating¹².

Even though there are numerous methods for synthesis of the NPs, maintaining the stability of the magnetic nanoparticle without agglomeration or precipitation is a challenge. Due to high surface area to volume ratio resulting in the high surface energy on the nanoparticles and in order to reduce the high energy, the particles tend to agglomerate causing the low colloidal stability. This phenomenon will highly effect to MNPs application in biological system which will be used in aqueous environment. Therefore, numerous materials have been studied to coat on the nanoparticles surface to improve their stability. The coating could be organic or inorganic such as surfactants¹³, polymer⁷, silica¹⁴, or carbon¹². Moreover, surface coating will give benefit for further conjugation with molecules of interest for example, SPIONs were coated with silica and modified surface to have carboxylic group for conjugated with amylase¹⁵ or coating with PEG and conjugated with folic acid for cancer targeting¹⁶.

The MNPs have been used in many applications including biomedical and biotechnological areas. In biomedical area, MNPs have been used in hyperthermia, magnetic resonance imaging (MRI), cellular therapy and labelling, gene and drug delivery⁹. In the biotechnological research, the nanomaterials can be used for bio-separation, biosensing, or

biocatalysis. The superparamagnetic nanoparticles have been promising nanomaterials in these applications because they are low-cost, scalability, and biocompatibility especially in complex biological environment. Even though there are numerous applications of using magnetic nanoparticles, in this research project, we will focus on bio-separation application for medical purpose, specifically to use such NPs for isolating biomarker protein from complex protein environment in blood serum. American Society of Clinical Oncology (ASCO) developed a guideline on using biomarker to guide treatment for breast cancer patients. The current biomarkers such as cancer antigen 15-3 (CA15-3), cancer antigen 27.29 (CA27.29) and carcinoembryonic antigen (CEA) which could be found in blood however, the elevated of these antigens could come from other conditions that not related with cancer as well. Therefore, using combination of biomarker would be better for the doctor to use as a guideline for treatment of patients or early diagnosis.

This biomarker protein is a riboflavin carrier protein (RCP) which has evidence to show that it is significantly elevated in cancer patients such as breast cancer, hepatocellular cancer, prostate cancer²⁻⁴. For example, in breast cancer patient, the RCP level in patient serum is about 3-4 fold higher than the healthy group and the RCP level is also related with the progression of the disease². Therefore, RCP could play important role in early detection of such cancers.

The potential of using nanoparticles and riboflavin carrier protein in cancer therapy have been explored. The nanoparticles were functionalized with riboflavin (Rf) which is a ligand for RCP. It has been shown that the RCP bind to Rf-functionalized nanoparticles and facilitates the uptake of the RCP-Rf-NP into cancer cells. For example, Rf was conjugated with the fifth generation (G5) poly(amidoamine) (PAMAM) dendrimer and showed that it can be targeted to deliver anticancer drug methotrexate (MTX) to KB cancer cells via Rf receptor mediated mechanism¹⁷. In addition, the conjugated Rf-PAMAM was further studied and it was shown that chemically modified Rf at N-3 position at an isoalloxazine head gave about 5 times lower K_D than chemically modified at a (D)-ribose unit attached at the N-10 position by isothermal titration calorimetry (ITC) and differential scanning calorimetry (DSC) methods¹⁸. Atomic Force Microscopy technique was also used to investigate the interaction between G5(Rf)-gold nanoparticles and the RCP by detecting the changes in particle height distribution¹⁹. This method serves as a quantitative analysis to monitor the nanoscale interaction between the Rf functionalized NPs and the RCP.

Moreover, the Rf was conjugated to N-(2-hydroxypropyl)methacrylamide (HPMA) copolymer and served as a targeting agent for delivering mitomycin C (MMC) to human breast cancer both MCF-7 and SKBR-3 cells²⁰. Not only the copolymer nanoparticles have been used for cancer therapy, the Ultrasmall Super Paramagneic Iron Oxide nanoparticles (USPIONs) have also been studied for the cancer therapy by functionalizing the USPIONs with flavin mononucleotide (FMN) as a specific target to cancer cells (PC-3) and activated endothelial cells (HUVEC)²¹. It showed high specific uptake by both PC-3 and HUVEC cells and due to their high T2-relaxivity, it can be used as a tool for molecular MRI.

Even though there are increasing number of research in utilizing the riboflavin system for development of drug delivery to cancer, there is so far no evidence of using riboflavin-nanoparticle complex for early cancer diagnose application. Therefore, this research will be an essential step and important knowledge for future development of nanomaterials for RCP serum detection which will be greatly benefit to early cancer diagnose. The conventional RCP determination is using radioimmuno assay (RIA) method which is very sensitive and highly specific however it is unsafe, requires high precaution and licensing because the involvement of radioactive compounds². It has been shown that applying magnetic nanoparticles for separation could give higher performance in detection of serum glycipan-3 which is highly expressed in hepatocellular carcinoma than the RIA method in term of linear range, limits of detection and total assay time²². Therefore, this development of Rf-SPIONs could have great potential to be used for separation, identification and quantitating RCP which could be easier, faster and safer than using the radioactive compound and would be an excellent alternative method for RCP detection. It also provides outstanding applicability in other tumor marker detections.

1.3 Objectives

- 1.3.1 To prepare various stable and biocompatible riboflavin functionalized magnetic nanoparticles (different size and different amount of riboflavin).
- 1.3.2 To understand the binding affinity and biophysical interaction between different amounts of ligands and riboflavin carrier proteins.
- 1.3.3 To understand the binding affinity and biophysical interaction between different surface coating on nanoparticles and riboflavin carrier proteins.
- 1.3.4 To investigate on the specificity and sensitivity of Rf-SPIONs to RCP.

1.4 Methodology

This project comprises interdisciplinary effort of nanoparticle preparation, physicochemical properties of the nanoparticles and the riboflavin carrier protein.

1.4.1 Purification of riboflavin carrier protein

Riboflavin carrier protein (RCP) will be purified from chicken white egg using column chromatography.

1.4.2 Synthesis of uncoated SPIONs (B-SPIONs)

FeCl $_2$ ·4H $_2$ O and FeCl $_3$ ·6H $_2$ O were dissolved in water. The mixture was heated to 80 $^{\circ}$ C with vigorous stirring under a N $_2$ atmosphere. NH $_4$ OH was added to the solution which rapidly changed the color to black. The reaction was maintained at this temperature for 10 minutes. The NPs were washed several times with water by magnetic decantation and redispersed in water as stock solution.

1.4.3 Synthesis of poly(methacrylic acid) (PMAA)-coated SPIONs (P-SPIONs)

B-SPIONs stock solution was dispersed in water and SDS was added, then the solution was stirred and heated to 70 $^{\circ}$ C followed by addition of neat MAA. After 45 minutes, $K_2S_2O_8$ solution was added, and the solution was further stirred for 2 hours. The NPs were washed several times with water to remove excess coating agents and then separated by magnetic decantation and dried in an oven for subsequent characterization.

1.4.4 Synthesis of citrate-coated SPIONs (C-SPIONs)

 $\rm FeCl_2\cdot 4H_2O$ and $\rm FeCl_3\cdot 6H_2O$ were dissolved in water and refluxed at 70 °C under $\rm N_2$ atmosphere with vigorous stirring for 30 minutes. $\rm NH_4OH$ was added and the reaction was maintained at this temperature for another 30 minutes. Tri-sodium citrate dihydrate solution was added and the temperature was raised to 90 °C for 1 hour. The resulting C-SPIONs were washed with water and separated by magnetic decantation and then redispersed in water as stock solution.

1.4.5 Synthesis of riboflavin-citrate ester (CARf)

Riboflavin and citric acid were dissolved in phenol and the reaction was heated to reflux condition at 140 $^{\circ}$ C. The reaction was prolonged for 4 hours then was cooled down to room

temperature. The resulting ester was isolated by precipitation in diethyl ether followed by vacuum filtration and was used as crude product without further purification.

1.4.6 Coating of SPIONs with CARf

B-SPIONs and riboflavin-citrate ester were mixed in water and stirred under $\rm N_2$ atmosphere at 90 $^{\rm o}$ C for 90 minutes. The resulting Rf-SPIONs were washed with water and isolated using magnetic decantation.

1.4.7 SPIONs characterization

Functional groups and surface coatings of the particles were studied by infrared spectrometry (Perkin Elmer Frontier FTIR spectrometer and Bruker ALPHA FTIR spectrometer). The particle size and morphology were analyzed using a transmission electron microscope (FEI Tecnai T20, USA). Bound proteins formed in coronas were analyzed by SDS-polyacrylamide gel electrophoresis (SDS-PAGE).

1.4.8 Investigation of colloidal stability in biological-relevant media

The synthesized SPIONs and coronas were suspended in water, PBS, DMEM, DMEM with 10% FBS, RPMI or RPMI with 10% FBS. Size and zeta potential were measured at different times of incubation to determine the stability of the particles in each medium using a Nanosizer 90 ZS (Malvern Instrument, UK).

1.4.9 Binding of Rf-SPIONs with RCP

Binding affinity of Rf-SPIONs with RCP was measured using Isothermal Titration Calorimetry (MicroCal PEAQ-ITC, Mavlvern Panalytical). Experiments were performed in 50 mM Tris buffer (pH 7.5) using following parameters: 25 $^{\circ}$ C, 750 rpm, 150 s between injections with 19 injections of 2 μ L each.

2. Results

2.1 SPIONs characterization

The synthesized B-SPIONs were irregular in shape with diameter ~6 nm when observed under transmission electron microscope (Figure 5). FTIR spectrum of B-SPIONs shows characteristic peak of Fe-O bonds at around 540 cm⁻¹. Broad peak at 3200 cm⁻¹ represents O-H stretching of hydroxyl groups. Coating of PMAA and citrate did not increase the size of SPIONs. The

coatings were confirmed by FTIR spectra. P-SPIONs shows C-H stretching peaks of PMAA at 2855 and 2924 cm⁻¹ with symmetrical stretching of carboxyl groups at 1400 cm⁻¹ (Figure 6).

Coating of B-SPIONs with CARf was confirmed by measuring fluorescence activity. The Rf-SPIONs shows broad fluorescence emission at \sim 524 nm when excited at 440 nm matching that of free riboflavin molecules.

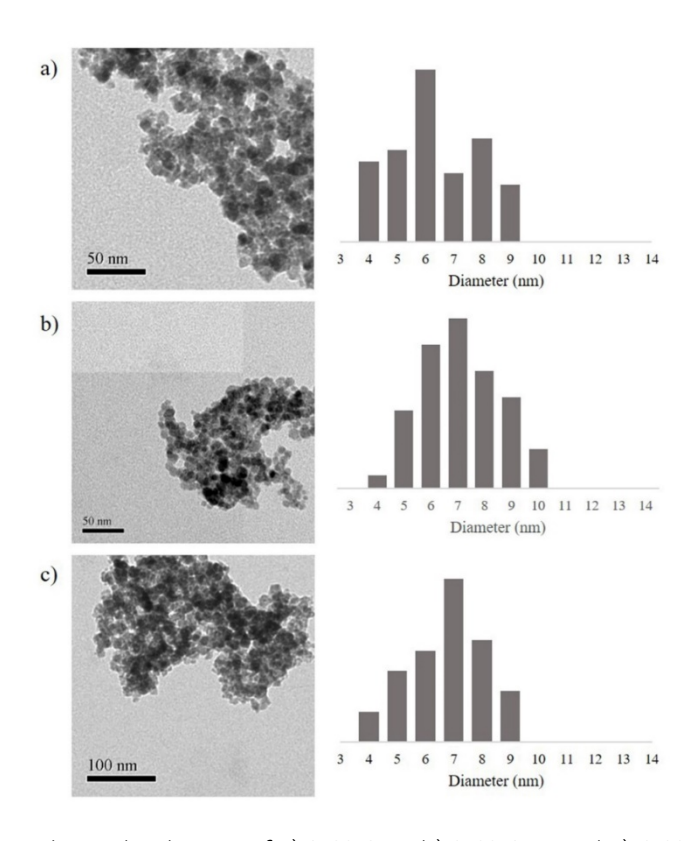


Figure 5. TEM images and size distribution of a) B-SPIONs, b) P-SPIONs and c) C-SPIONs.

2.2 Colloidal stability B-SPIONs, P-SPIONs and C-SPIONs were resuspended in commonly used biological media: water, PBS, DMEM, DMEM with 10% FBS, RPMI and RPMI with 10% FBS and the colloidal stability was evaluated by determination of the hydrodynamic size using dynamic light scattering (figure 7). The uncoated SPION showed rapid aggregation in water, giving a diameter >1 μ m (figure 7a). Surface modification of SPION with either PMAA or citrate resulted in a smaller hydrodynamic size (~100 nm) and maintained for at least 24 hours.

In PBS, B-SPIONs had an average diameter of \sim 500 nm (figure 7b), however after prolonged incubation for 24 hours, aggregation was observed resulting in an average particle diameter of size \sim 1 μ m, similar to what was observed in water. The sizes of the P-SPIONs and C-SPIONs were

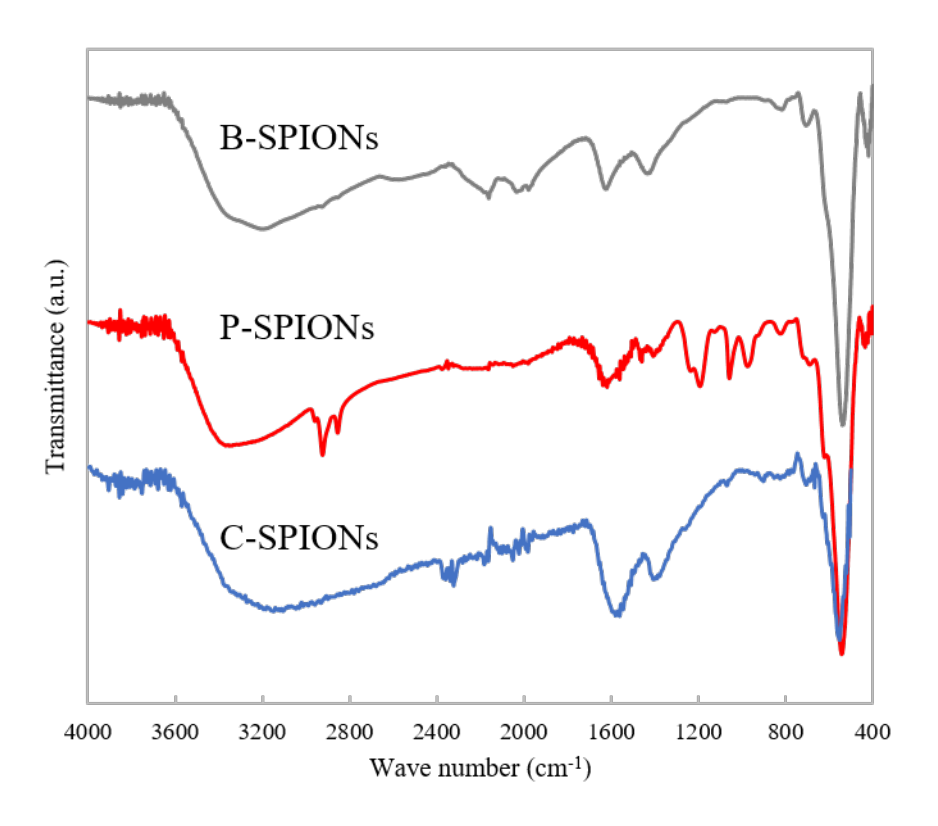


Figure 6. FTIR spectra of B-SPIONs, P-SPIONs and C-SPIONs.

 \sim 100 nm, however, after prolonged incubation in PBS, the size of C-SPIONs increased to \sim 300 nm, whereas the P-SPIONs remained the same size.

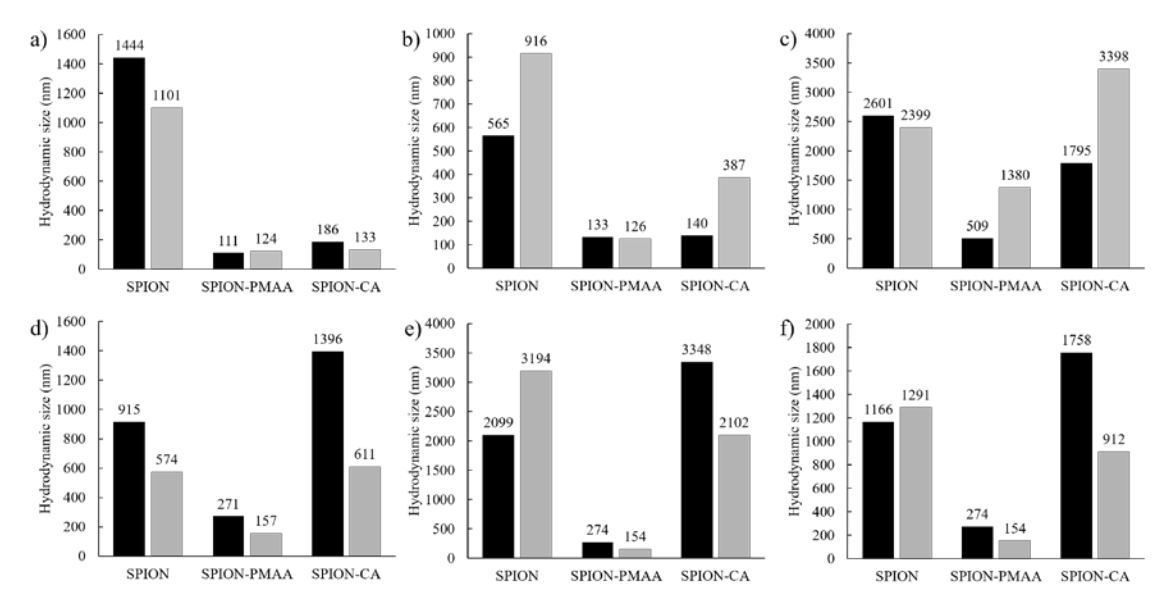


Figure 7. a)-f) Hydrodynamic diameters of B-SPIONs, P-SPIONs and C-SPIONs in water, PBS, DMEM, DMEM+10% FBS, RPMI and RPMI+10% FBS respectively. Black and grey bars represent 0 and 24 hours of incubation respectively.

In cell culture media, all samples were highly unstable resulting in aggregation with particle sizes >1 μ m (figure 7c). Surprisingly, addition of FBS to the culture medium significantly reduced the sizes of all samples especially SPION-PMAA for which the hydrodynamic size decreased from 1 μ m to ~100 nm (figure 7d-f).

2.3 Binding of Rf-SPIONs with RCP

Binding of Rf-SPIONs with RCP was studied using ITC technique. The riboflavin-conjugated SPIONs showed binding signature when titrated with RCP solution. Dissociation constant (K_D) between the particles and RCP was around 13 μ M which is higher than that of free riboflavin (127 nM). Control experiments were performed by titrating of B-SPIONs with RCP and Rf-SPIONs with bovine serum albumin (BSA) which both showed no binding activity.

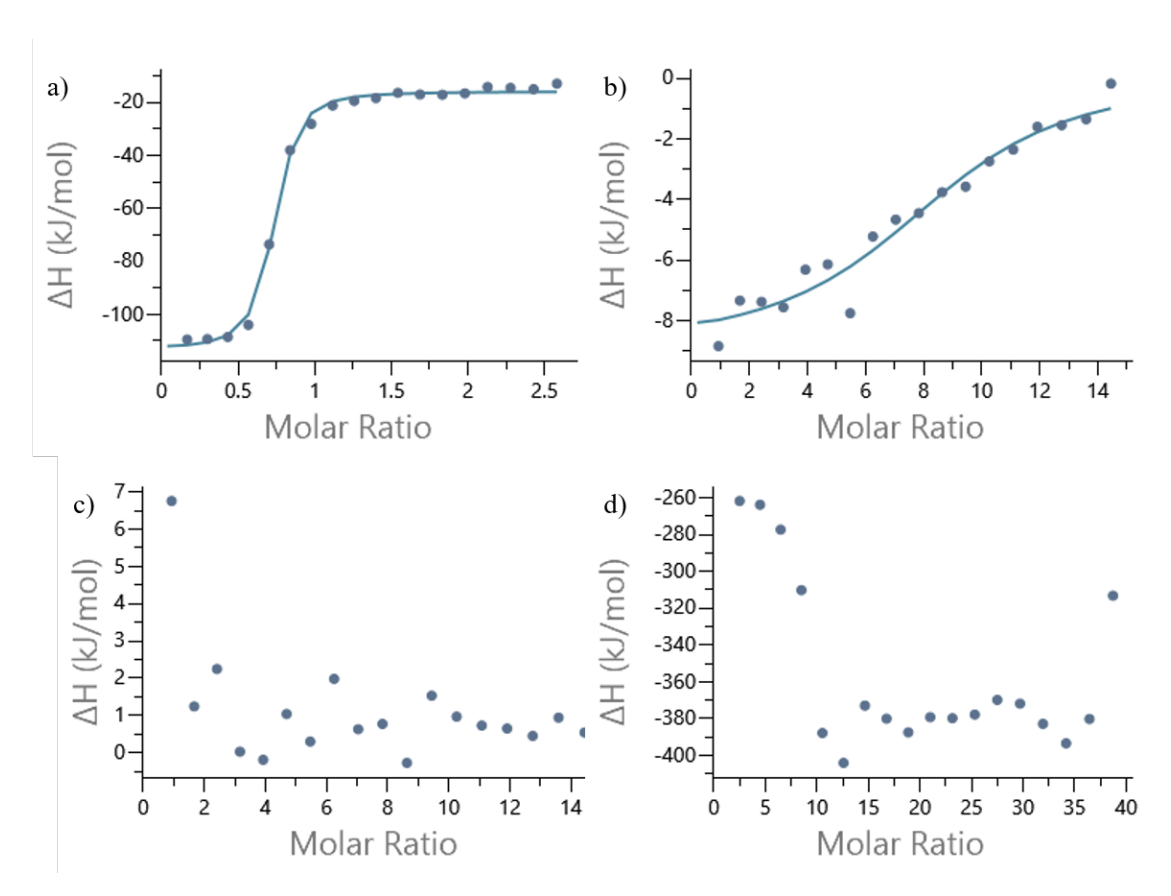


Figure 8. Integrated heat plot of binding between a) free riboflavin and RCP, b) Rf-SPIONs and RCP, c) Rf-SPIONs and BSA and d) B-SPIONs and RCP.

3. Conclusion and Discussion

The synthesized B-SPIONs were successfully coated with PMAA and citrate molecules as evidenced from FTIR spectra. Peaks at around 1400 and 1600 cm⁻¹ of both P-SPIONs and C-SPIONs represent symmetric stretching and vibration mode carboxyl groups which suggest symmetrical chelation of carboxyl groups of PMAA and citrate with SPIONs surface²³. The coatings did not significantly increase the size of SPIONs but provided more spherical surface especially for P-SPIONs as observed from TEM images.

Riboflavin was conjugated to citric acid through refluxing in phenol. The riboflavin-citrate ester was mixed with B-SPIONs to yield Rf-SPIONs with riboflavin moiety as ligand. The riboflavin-citrate ester was expected to bind to SPIONs surface through carboxylic groups in similar manner as citrate molecules. The coating was confirmed by fluorescent emission of the NPs at \sim 524 nm when excited at 440 nm. In addition, CARf molecules also provide surface stabilization as Rf-SPIONs showed hydrodynamic diameter of \sim 100 nm while uncoated B-SPIONs showed size of \sim 1 μ m.

Binding of Rf-SPIONs was studied using ITC technique. The Rf-SPIONPs showed binding with RCP with K_D of ~13 μ M. High K_D values indicate weak binding between ligands and enzymes. RCP binds strongly to free riboflavin with K_D as high as 127 nM. The weaker binding between Rf-SPIONs and RCP when compared to free riboflavin ligands could be due to steric hindrance of the short ligand preventing successful binding. Specificity between Rf-SPIONs and RCP was confirmed by control experiments. Titration of Rf-SPIONs with BSA showed no binding similar to titration of B-SPIONs with RCP.

To conclude, SPIONs were synthesized and their stability in biological environment was studied and enhanced by coating with either PMAA polymer or citrate molecules. Citrate was further conjugated with riboflavin molecules and used as stabilizing agents with riboflavin terminal available for RCP binding. The Rf-SPIONs were confirmed to bind specifically to RCP with K_D of 13 μ M. The specificity of Rf-SPIONs with RCP suggest potential use of the material as tool for separation of RCP. However, improvement of the ligands for lower K_D value or stronger binding might be needed for further effective uses.

4. Output

4.1 International conference

- Wid Mekseriwattana, Rattanaporn Kriangsaksri, Supreeya Srisuk, <u>Kanlaya</u>
 <u>Prapainop</u>. "Synthesis of Superparamagnetic Iron Oxide Nanoparticles (SPIONs)
 for biomedical applications". 1st MRS Thailand International Conference, 31
 October 3 November 2017, Chiangmai, Thailand (poster presentation).
- Wid Mekseriwattana, Supreeya Srisuk, Rattanaporn Kriangsaksri, Nuttawee Niamsiri, <u>Kanlaya Prapainop</u>. "Investigation of colloidal behavior of surface-modified superparamagnetic iron oxide nanoparticle under biological environment". 2018 International Conference on Nano Science and Technology, 24-26 August 2018, Sapporo, Japan (oral presentation).

4.2 Publication

- <u>Prapainop, K.</u>; Miao, R.; Aberg, C.; Salvati, A.; and Dawson, K. A. "Reciprocal upregulation of scavenger receptors complicates interpretation of nanoparticles uptake in non-phagocytic cells". *Nanoscale*. 2017, 9, 11261.
- Wid Mekseriwattana, Yotsakorn Tantiapibalkul, <u>Kanlaya Prapainop</u>. The preparation of superparamagnetic iron oxide nanoparticles for investigation of interaction between nanoparticles and cells. *ScienceAsia* (Under revision)
- Wid Mekseriwattana, Supreeya Srisuk, Ruttanaporn Kriangsaksri, Nuttawee Niamsiri, <u>Kanlaya Prapainop</u>. The impact of serum proteins and surface chemistry on magnetic nanoparticle colloidal stability and cellular uptake in breast cancer cells. An Official Journal of the American Association of Pharmaceutical Scientists (Under revision)

5. References

- 1. Yigit, M. V.; Moore, A.; Medarova, Z., Magnetic nanoparticles for cancer diagnosis and therapy. *Pharm Res* **2012**, *29* (5), 1180-8.
- 2. Rao, P. N.; Levine, E.; Myers, M. O.; Prakash, V.; Watson, J.; Stolier, A.; Kopicko, J. J.; Kissinger, P.; Raj, S. G.; Raj, M. H., Elevation of serum riboflavin carrier protein in breast cancer. *Cancer Epidemiol Biomarkers Prev* **1999**, *8* (11), 985-90.
- 3. Rao, P. N.; Crippin, J.; Levine, E.; Hunt, J.; Baliga, S.; Balart, L.; Anthony, L.; Mulekar, M.; Raj, M. H., Elevation of serum riboflavin carrier protein in hepatocellular carcinoma. *Hepatol Res* **2006**, *35* (2), 83-7.

- 4. Johnson, T.; Ouhtit, A.; Gaur, R.; Fernando, A.; Schwarzenberger, P.; Su, J.; Ismail, M. F.; El-Sayyad, H. I.; Karande, A.; Elmageed, Z. A.; Rao, P.; Raj, M., Biochemical characterization of riboflavin carrier protein (RCP) in prostate cancer. *Front Biosci-Landmrk* **2009**, *14*, 3634-40.
- 5. Lu, A.-H.; Schmidt, W.; Matoussevitch, N.; Bönnemann, H.; Spliethoff, B.; Tesche, B.; Bill, E.; Kiefer, W.; Schüth, F., Nanoengineering of a magnetically separable hydrogenation catalyst. *Angew Chem Int Ed* **2004**, *43* (33), 4303-4306.
- 6. Arai, S.; Okochi, M.; Shimizu, K.; Hanai, T.; Honda, H., A single cell culture system using lectin-conjugated magnetite nanoparticles and magnetic force to screen mutant cyanobacteria. *Biotechnol Bioeng* **2016**, *113* (1), 112-9.
- 7. Barrow, M.; Taylor, A.; Murray, P.; Rosseinsky, M. J.; Adams, D. J., Design considerations for the synthesis of polymer coated iron oxide nanoparticles for stem cell labelling and tracking using MRI. *Chem Soc Rev* **2015**, *44* (19), 6733-48.
- 8. Takafuji, M.; Ide, S.; Ihara, H.; Xu, Z. H., Preparation of poly(1-vinylimidazole)-grafted magnetic nanoparticles and their application for removal of metal ions. *Chem Mater* **2004**, *16* (10), 1977-1983.
- 9. Thomas, R.; Park, I. K.; Jeong, Y. Y., Magnetic iron oxide nanoparticles for multimodal imaging and therapy of cancer. *Int J Mol Sci* **2013**, *14* (8), 15910-30.
- 10. Lu, A. H.; Salabas, E. L.; Schuth, F., Magnetic nanoparticles: synthesis, protection, functionalization, and application. *Angew Chem Int Ed* **2007**, *46* (8), 1222-44.
- 11. Lee, K. S.; Lee, I. S., Decoration of superparamagnetic iron oxide nanoparticles with Ni²⁺: agent to bind and separate histidine-tagged proteins. *Chem Commun* **2008**, (6), 709-711.
- 12. Lu, A. H.; Li, W. C.; Matoussevitch, N.; Spliethoff, B.; Bonnemann, H.; Schuth, F., Highly stable carbon-protected cobalt nanoparticles and graphite shells. *Chem Commun (Camb)* **2005**, (1), 98-100.
- 13. Shen, L.; Laibinis, P. E.; Hatton, T. A., Bilayer surfactant stabilized magnetic fluids: synthesis and interactions at interfaces. *Langmuir* **1999**, *15* (2), 447-453.
- 14. Lu, Y.; Yin, Y.; Mayers, B. T.; Xia, Y., Modifying the surface properties of superparamagnetic iron oxide nanoparticles through a sol–gel approach. *Nano Lett* **2002**, *2* (3), 183-186.
- 15. Guo, H.; Tang, Y.; Yu, Y.; Xue, L.; Qian, J. Q., Covalent immobilization of alpha-amylase on magnetic particles as catalyst for hydrolysis of high-amylose starch. *Int J Biol Macromol* **2016**, *87*, 537-44.
- 16. Esfandyari-Manesh, M.; Darvishi, B.; Ishkuh, F. A.; Shahmoradi, E.; Mohammadi, A.; Javanbakht, M.; Dinarvand, R.; Atyabi, F., Paclitaxel molecularly imprinted polymer-PEG-folate nanoparticles for targeting anticancer delivery: characterization and cellular cytotoxicity. *Mater Sci Eng C* **2016**, *62*, 626-33.
- 17. Thomas, T. P.; Choi, S. K.; Li, M.-H.; Kotlyar, A.; Baker Jr, J. R., Design of riboflavin-presenting PAMAM dendrimers as a new nanoplatform for cancer-targeted delivery. *Bioorganic & Medicinal Chemistry Letters* **2010**, *20* (17), 5191-5194.

- 18. Witte, A. B.; Timmer, C. M.; Gam, J. J.; Choi, S. K.; Banaszak Holl, M. M.; Orr, B. G.; Baker, J. R.; Sinniah, K., Biophysical characterization of a riboflavin-conjugated dendrimer platform for targeted drug delivery. *Biomacromolecules* **2012**, *13* (2), 507-16.
- 19. Witte, A. B.; Leistra, A. N.; Wong, P. T.; Bharathi, S.; Refior, K.; Smith, P.; Kaso, O.; Sinniah, K.; Choi, S. K., Atomic force microscopy probing of receptor-nanoparticle interactions for riboflavin receptor targeted gold-dendrimer nanocomposites. *J Phys Chem B* **2014**, *118* (11), 2872-82.
- 20. Bareford, L. M.; Avaritt, B. R.; Ghandehari, H.; Nan, A.; Swaan, P. W., Riboflavin-targeted polymer conjugates for breast tumor delivery. *Pharm Res* **2013**, *30* (7), 1799-812.
- 21. Jayapaul, J.; Hodenius, M.; Arns, S.; Lederle, W.; Lammers, T.; Comba, P.; Kiessling, F.; Gaetjens, J., FMN-coated fluorescent iron oxide nanoparticles for RCP-mediated targeting and labeling of metabolically active cancer and endothelial cells. *Biomaterials* **2011**, *32* (25), 5863-71.
- Zhang, Q. Y.; Chen, H.; Lin, Z.; Lin, J. M., Chemiluminescence enzyme immunoassay based on magnetic nanoparticles for detection of hepatocellular carcinoma marker glypican-3. *J Pharm Anal* **2011**, *1* (3), 166-174.
- 23. Nigam, S.; Barick, K. C.; Bahadur, D., Development of citrate-stabilized Fe_3O_4 nanoparticles: conjugation and release of doxorubicin for therapeutic applications. *J Magn Magn Mater* **2011**, *323* (2), 237-243.



Nanoscale



PAPER

View Article Online
View Journal | View Issue



Cite this: Nanoscale, 2017, 9, 11261

Reciprocal upregulation of scavenger receptors complicates interpretation of nanoparticle uptake in non-phagocytic cells†

Kanlaya Prapainop, b ‡ Rong Miao, $\S^{a,b}$ Christoffer Åberg, b ¶ Anna Salvati b ¶ and Kenneth A. Dawson*

Nanoparticles have great potential as drug delivery vehicles or as imaging agents for treatment and diagnosis of various diseases. It is therefore crucial to understand how nanoparticles are taken up by cells, both phagocytic and non-phagocytic. Small interference RNA has previously been used to isolate the effect of particular receptors in nanoparticle uptake by silencing their expression. Here we show that, when it comes to receptors with overlapping function, interpretation of such data has to be done with caution. We followed the uptake of silica nanoparticles by scavenger receptors in A549 lung epithelial cells. While we successfully knocked-down gene expression of several different receptors within the scavenger receptor family (SR-A1, MARCO, SR-BI, LOX-1 and LDLR) this caused reciprocal up and down regulation of the other scavenger receptors. Subsequent nanoparticle uptake experiments in silenced cells exhibit a complex behaviour, which could easily be misinterpreted if reciprocal regulation is not considered. Preliminary identification of the actual scavenger receptors involved can be found by disentangling the effects mathematically. Finally, we show that the effects are still present under more realistic biological conditions, namely at higher serum concentrations.

Received 8th May 2017, Accepted 19th July 2017 DOI: 10.1039/c7nr03254d

rsc.li/nanoscale

Introduction

Nanoparticles are promising in medical applications, both as drug delivery vectors and for diagnosis. However, despite numerous synthesized nanoparticles exhibiting excellent targeting in *in vitro* studies, successful translation to the clinic has been more limited and the majority of nanoparticles do not reach their desired target. Therefore understanding the fundamental science of how nanoparticles interact with cells

enhanced efficacy.² Most nanoparticles readily enter cells and interact with the cellular machinery using energy-dependent processes.³ This is particularly so in the case of the mononuclear phagocyte system,⁴ a fact that hinders the potential for using nanoparticles as drug delivery vehicles. Nanoparticle uptake can be described in terms of an initial adhesion of the nanoparticle to the cell membrane followed by internalisation of the nanoparticle into the cell⁵ and subsequent trafficking to different subcellular locations. Which receptors and uptake pathways are involved in the internalisation is, however, still largely unsettled.

is an essential step towards improved nanoparticle design for

Scavenger receptors (SRs) are transmembrane proteins of at least eight different subclasses (A–H). Class A scavenger receptors are widely expressed on macrophages⁶ and two of the major subtypes, scavenger receptor AI/II and macrophage receptor with collagenous structure (MARCO), have been found to facilitate the uptake of nanoparticles.^{7–9} Also scavenger receptors of class B have been reported to be involved in the uptake of nanoparticles.¹⁰ Here we focus on how scavenger receptors mediate the uptake of amorphous silica (SiO₂) nanoparticles in non-phagocytic A549 lung epithelial cells. Consistent with the general observation, silica nanoparticles have been shown to be taken up by various cell types, including macrophages and lung epithelial cells.^{11–14} While several

^aCentre for BioNano Interactions, School of Chemistry and Chemical Biology and Conway Institute for Biomolecular and Biomedical Research, University College Dublin, Belfield, Ireland. E-mail: kenneth.a.dawson@cbni.ucd.ie;

Tel: +353 1 716 2459

^bTechnical Institute of Physics and Chemistry, Chinese Academy of Sciences, Beijing 100190, China

^cGroningen Biomolecular Sciences and Biotechnology Institute, University of Groningen, 9747 AG Groningen, The Netherlands

 $[\]dagger$ Electronic supplementary information (ESI) available: Supplementary tables and figures. See DOI: 10.1039/c7nr03254d

[‡]Current address: Department of Biochemistry, Faculty of Science, Mahidol University, Bangkok, Thailand.

[§] Current address: Key Laboratory of Applied Surface and Colloid Chemistry of Ministry of Education, Shaanxi Normal University, Xi'an 710062, People's Republic of China

[¶]Current address: Groningen Research Institute of Pharmacy, University of Groningen, Antonius Deusinglaan 1, 9713 AV Groningen, The Netherlands.

studies have specifically investigated the uptake of silica nanoparticles *via* scavenger receptors in phagocytic cells^{7,15-17} here we set out to understand the role of scavenger receptors in non-phagocytic lung epithelial cells, using A549 cells as a model system. A549 are human lung carcinoma epithelial cells which can be grown in adhesion *in vitro*.

Small interference RNA (siRNA) has been used as a tool for studying the role of specific receptors in nanoparticle uptake. 18,19 For example, we have previously synthesized transferrin-functionalized nanoparticles whose uptake into cells was lowered upon silencing the transferrin receptor, suggesting that those nanoparticles do, indeed, target the transferrin receptor. 18 Naturally, knowing a particle is recognised by a receptor does not imply full knowledge of the subsequent internalisation mechanism. Nevertheless, it constitutes essential information on the very first step of the uptake process. Here we use siRNA silencing for scavenger receptormediated uptake of silica nanoparticles. However, for receptors within a family that share function, selective knock-down can cause difficult to predict effects on other receptors within the family. We demonstrate this within the scavenger receptor family and show the complex behaviour of nanoparticle uptake that ensues and the complications that arise in interpreting the behaviour.

Results and discussion

A549 lung epithelial cells express scavenger receptors such as SR-A, MARCO, SR-BI, LOX-1 and LDLR (Table S2†). The level of transcripts specific for SR-BI is higher than other scavenger receptors, as previously reported in human bronchial epithelial cells. RNA interference was introduced to knockdown the expression of several scavenger receptors in A549 cells. Two separate duplexes of validated siRNAs, targeting separate regions of the target mRNA, were used (Table S1†). The efficiency of gene silencing was determined by measuring the relative reduction in scavenger receptor expression using qPCR (Fig. S1†). The siRNA with the highest efficiency of silencing each respective scavenger receptor was selected for the further experiments.

As model systems, different sizes of fluorescent silica nanoparticles (10, 50 and 200 nm) were used to investigate the effect of nanoparticle size in their uptake mechanisms by scavenger receptors. The nanoparticles were synthesised as described previously, with a silica core surrounded by an arginine shell that prevents dissolution. Basic size characterization by dynamic light scattering of the nanoparticles dispersed in the relevant media is presented in Table S3.† In serum-free MEM the silica nanoparticles exhibit sizes of about 18, 59 and 240 nm, that is, roughly the intended sizes. However, upon dispersion in serum-containing medium (10%, 30% and 50%) the average size of the 10 and 50 nm nanoparticles increases substantially, most likely due to nanoparticle agglomeration. The 200 nm nanoparticles, in contrast, remain mostly well-dispersed. In what follows we

will nevertheless refer to the nanoparticles by their intended sizes.

In general, silica nanoparticles are known to enter cells, including the A549 cells used here, and extensive information is already available on their intracellular behaviour and final fate inside cells.^{5,11,22} This is also true for the specific silica particles, and variations thereof, we employ here. 18,21,23 In order to determine whether these nanoparticles are taken up by scavenger receptors, polyinosinic acid (poly I), a known non-specific scavenger receptor ligand, was used to block uptake by scavenger receptors; polycytidylic acid (poly C) was used as a negative control (Fig. 1A). Cellular uptake of the 50 and 200 nm nanoparticles was decreased after pre-incubation with poly I, but not with the negative control poly C; however, the uptake of the 10 nm nanoparticles was unchanged (Fig. 1A) even as the concentration of poly I was increased up to 500 μg ml⁻¹ (Fig. S2†). This selective inhibition of nanoparticle uptake by poly I suggests that the uptake of the 50 and 200 nm silica nanoparticles is mediated by scavenger receptors, while the 10 nm nanoparticles might be taken up by different mechanism(s).

We next explored the role of each scavenger receptor in nanoparticle uptake by using cells silenced for specific scavenger receptors (Fig. 1B–D). Surprisingly, most of the silenced cells do not show a reduction of nanoparticle uptake, but rather uptake is *increased* after silencing scavenger receptors. The only exception is LDLR silenced cells, which showed lower uptake of the silica nanoparticles (of all sizes) after silencing. Notably, in LOX-1 silenced cells, the 50 and 200 nm nanoparticles are taken up to a much higher extent than in control cells (Fig. 1C and D).

Even though the uptake mechanism seems to be complex, we further investigated whether the uptake of silica nanoparticles in cells silenced for a particular scavenger receptor (SR-A, SR-BI, MARCO, LOX-1 or LDLR) is due to other scavenger receptors. The silenced cells were thus pre-incubated with the non-specific scavenger receptor inhibitor poly I (again using poly C as a control) prior to exposure to the 50 and 200 nm silica nanoparticles. In all cases, uptake is reduced by pre-incubation with inhibitor, but not with negative control (Fig. 1E and F). Using fucoidan as a scavenger receptor inhibitor gives the same outcome (Fig. S3†). The results suggest that the increased uptake in cells silenced for a particular receptor is possibly due to the up-regulation of one of the other non-silenced scavenger receptors.

To validate the hypothesis that up-regulation of other scavenger receptors is the cause of increased uptake after silencing a given scavenger receptor, we further investigated how the expression of the other scavenger receptors were affected by silencing a specific receptor (Fig. 2). The results show that, though we successfully knocked down the mRNA expression level of each individual scavenger receptor, silencing a specific scavenger receptor not only reduces the mRNA expression level of the receptor of interest, but can also lead to up- or down-regulation of the other receptors. For example, silencing the SR-A receptor, while reducing the mRNA expression level of

Nanoscale

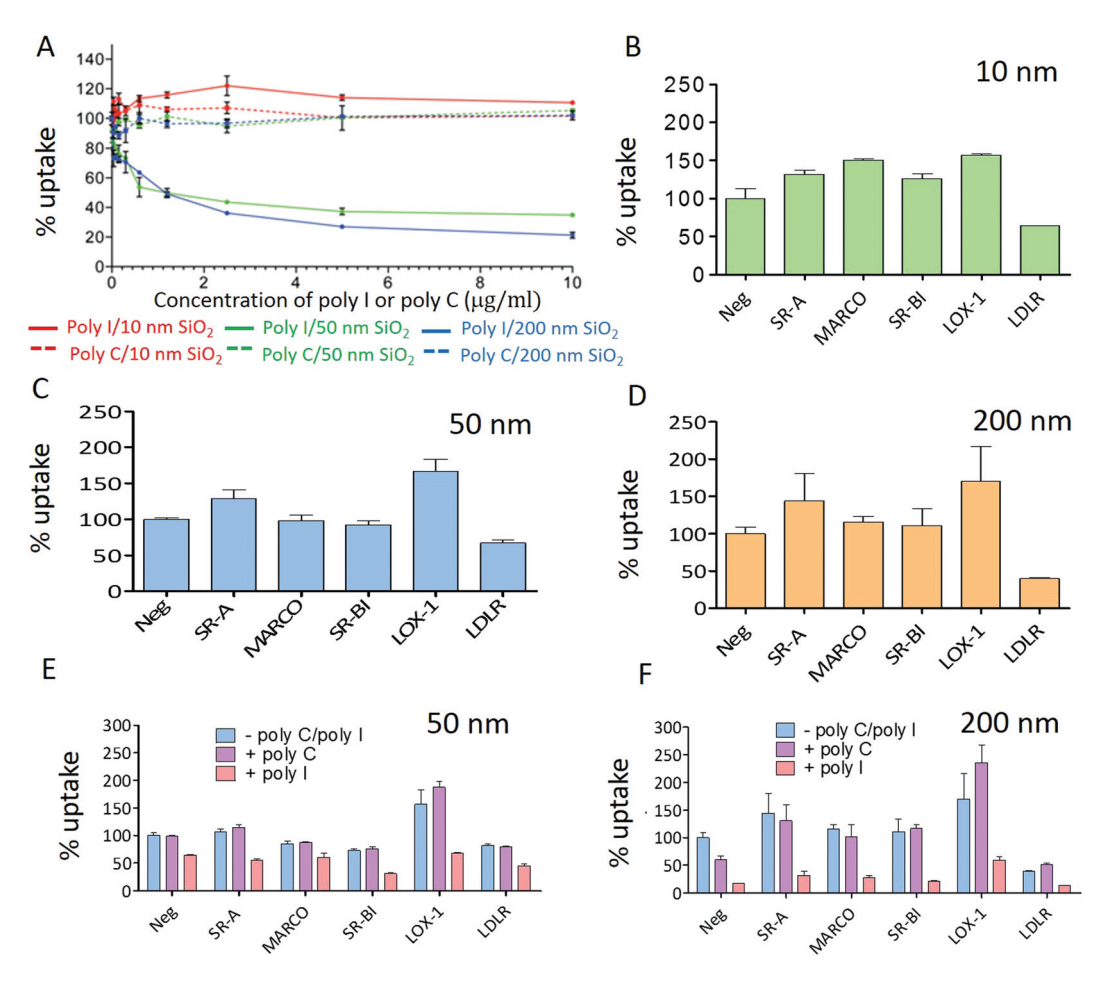


Fig. 1 Role of scavenger receptors in cellular uptake of silica nanoparticles in A549 cells. (A) Nanoparticle uptake after pre-incubation with inhibitor as a function of inhibitor concentration. Cells were pre-incubated with either poly I (inhibitor) or poly C (negative control) at different concentrations for 30 min before being exposed for 3 h to 100 μ g mL $^{-1}$ of 10, 50 and 200 nm silica nanoparticles dispersed in 10% foetal bovine serum. Results are presented as the median cell fluorescence intensity (MFI) due to nanoparticle uptake relative to cells without pre-incubation with inhibitor. (B-D) Nanoparticle uptake in A549 cells silenced for the scavenger receptors SR-A, MARCO, SR-BI, LOX-1 and LDLR or negative silencer control (Neg). Cells were silenced for 72 h before exposure for 3 h to 100 µg mL⁻¹ of (B) 10 nm, (C) 50 nm and (D) 200 nm silica nanoparticles dispersed in 10% foetal bovine serum. (E-F) Nanoparticle uptake in scavenger receptor silenced cells pre-incubated with inhibitor. A549 cells were silenced for 72 h as above and then pre-incubated with either poly I or poly C (5 μ g ml⁻¹) for 30 min prior to exposure for 3 h to 100 μ g mL⁻¹ (E) 50 nm or (F) 200 nm silica nanoparticles.

SR-A to 30%, also up-regulates the MARCO, LOX-1 and LDL receptors (Fig. 2A). In contrast, silencing the MARCO receptor causes down-regulation not only of MARCO, but concomitantly induces the down-regulation of SR-A, SR-BI and LOX-1 (Fig. 2B). Furthermore, Fig. 2C shows that silencing SR-BI decreases the expression of all investigated receptors (SR-A, MARCO and LDLR) except LOX-1, which is up-regulated. Interestingly, in LOX-1 silenced cells, the MARCO receptor is up-regulated 3 fold compared to control cells, while SR-BI and LDLR are unaffected (Fig. 2D). In LDLR silenced cells, the knockdown causes up-regulation of LOX-1 but down-regulation of SR-A and MARCO (Fig. 2E). This reciprocal up-regulation was also previously observed upon silencing SR-A and CD36 in mouse macrophage RAW 264.7 cells.²⁴ Overall, these results suggest partly overlapping functions and sensitive regulation to balance the function of these receptors.

Based on these results, the origin of the complicated behaviour of the uptake under silenced conditions (Fig. 1C and D) is clear. For example, the lowered uptake of silica nanoparticles in LDLR silenced cells (Fig. 1C and D) do not simply mean that the LDLR receptor is the major player in their cellular uptake, because other scavenger receptors (SR-A and MARCO) are also down-regulated (Fig. 2E). Conversely, up-regulation of a receptor in cells silenced for a certain receptor could also enhance the uptake of nanoparticles into those cells. Therefore, if siRNA is used to reduce the expression of a particular receptor and there is no change in nanoparticle uptake behaviour, it does not necessarily imply that the receptor is not involved in the uptake mechanism because the cells might compensate the lack of that particular receptor by overexpression of others. Hence interpretation of results from knockdown gene expression has to be done with caution.

Paper Nanoscale

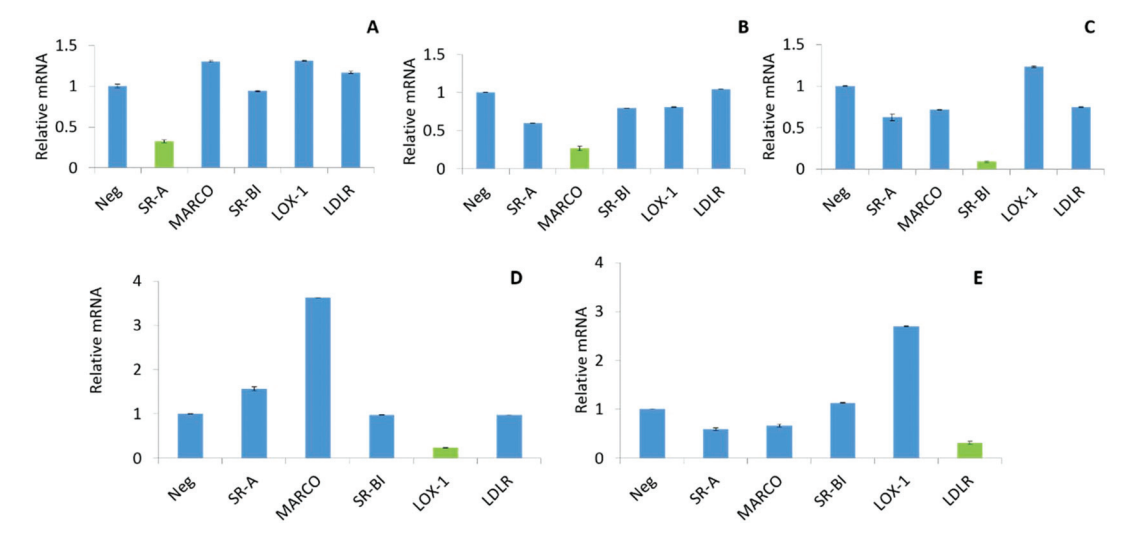


Fig. 2 Expression levels of several scavenger receptors upon silencing a specific receptor. (A) SR-A; (B) MARCO; (C) SR-BI; (D) LOX-1 and (E) LDLR were silenced and the mRNA expression levels of all the indicated receptors determined using qPCR. Results are presented as the mRNA quantity relative to negative control (Neg) and the scavenger receptor intended to be silenced is shown in green.

Nevertheless, we can attempt to understand the behaviour to some extent by considering the effect that silencing one receptor has on the expression of the other receptors (Fig. 2) and correlating that with the uptake (Fig. 1C and D). For example, silencing LDLR causes a substantial increase in the expression of LOX-1, while none of the other receptors are upregulated (Fig. 1E). However, uptake of nanoparticles into LDLR silenced cells is not higher than control cells, neither for the 50 nm nor for the 200 nm silica nanoparticles (Fig. 1C and D, respectively). This could suggest that LOX-1 is not involved in the uptake of the 50 and the 200 nm silica nanoparticles. As another example, silencing of LOX-1 causes a substantial up-regulation of MARCO (Fig. 2D) with a concomitant increase in the uptake for both the 50 and the 200 nm silica nanoparticles (Fig. 1C and D, respectively). This could suggest that MARCO is involved in their uptake.

We may take this one step further by using a simple mathematical model to perform such considerations "automatically". We now illustrate the basic idea behind such an approach. Thus let J be the total flux, via all pathways, of nanoparticles into cells. This flux is not directly measured (in these experiments), but for the exposure times reported here (Fig. 1) we may assume that the cellular fluorescence due to nanoparticle uptake is roughly proportional to this flux, i.e., fluorescence $\approx J \times \text{time}$. The underlying assumption is that after some time the initial transient, due to nanoparticles adsorbing to the outer cell membrane, is negligibly small compared to the number of nanoparticles inside the cell, something we have previously shown to be the case.⁵ Furthermore, 3 h is still short compared to the diluting process of cell division which takes place at time-scales of days, again something we have shown previously.25 Thus, the total flux is, in essence, measurable and may be approximated with the results shown in Fig. 1C-E.

We now write the total flux into cells as the sum of fluxes via all the different pathways

$$J = \sum_i j_{{
m SR},i} N_{{
m SR},i} + J'$$

where the first term represents the fluxes due to the receptors explicitly studied here, and the second term the flux, J', due to all other pathways. $N_{SR,i}$ is the number of receptors of the scavenger receptor type i, and $j_{SR,i}$ is the flux *per number* of such receptors. In non-silenced cells, we use the equation essentially as-is, *i.e.*,

$$J^{\mathrm{us}} - J^{'\mathrm{us}} = \sum_{i} j_{\mathrm{SR},i} N_{\mathrm{SR},i}^{\mathrm{us}}$$

where the superscript 'us' denotes 'unsilenced'. However, for silenced cells we rewrite the expression to

$$J^{\rm s} - J^{' \rm s} = \sum_{i} j_{{\rm SR},i} N_{{\rm SR},i}^{\rm us} \frac{N_{{\rm SR},i}^{\rm s}}{N_{{\rm SR},i}^{\rm us}}$$

where the superscript 's' denotes 'silenced'. The reason for this reformulation is that the expression now contains the ratio of the number of receptors in silenced to non-silenced cells, $N_{\text{SR},i}^{\text{s}}/N_{\text{SR},i}^{\text{us}}$, *i.e.*, the up/down-regulation of the receptor.

It is now possible to extract the flux via the measured scavenger receptors, $j_{SR,i}N_{SR,I}^{us}$, from the experimental data; that is, it is possible to extract via which receptors the particles enter under normal conditions. We use the data in Fig. 1E and F for the fluxes of the 50 and 200 nm silica nanoparticles, respectively. For the total flux, J, we use the average of the results with no blocking agent and with the negative control blocking agent (poly C); for the flux via other receptors, J', we use the results with blocking agent (poly I). The ratio of the number of receptors in silenced to non-silenced cells, $N_{SR,i}^{s}/N_{SR,i}^{us}$, we approximate with the mRNA expression levels measured

Nanoscale

(Fig. 2). Using all conditions, we then have 6 equations (unsilenced cells and 5 different silencing conditions) to extract 5 unknowns. We do this by least-square minimisation, with the added condition of the fluxes being positive, propagating the errors in the fluxes.

Fig. 3 shows the results. It suggests that the uptake of both particles occurs predominately via the MARCO and LDLR receptors, with some involvement of LOX-1 in the case of the 50 nm silica nanoparticles. The main weakness in this approach is that not all scavenger receptors have been included in the study, and it is possible that differential up/ down regulation of other scavenger receptors could also contribute. Uptake taking place via non-scavenger receptors does, however, not cause issues (as long those receptors are not blocked by poly I), because this has been excluded from the analysis by using the blocking experiments (Fig. 1E and F). Another concern is the relation between the actual number of receptors at the cell membrane and the mRNA levels measured (Fig. 2). Still, using the extracted receptor fluxes to predict (or, rather, postdict) the uptake under all measured conditions shows a reasonable description of the overall data (Fig. S4†). While further studies would be needed to confirm the conclusions, this exercise nevertheless shows the potential for extracting which receptors are involved in the uptake process from rather complex datasets.

To address whether the effects remain in more realistic biological environments (i.e., in the presence of higher amounts of serum), cells were exposed to silica nanoparticles dispersed in different amounts of serum and assessed for uptake as above (Fig. S5†). Addition of serum decreased the uptake of all nanoparticles, in particular the 200 nm silica nanoparticles

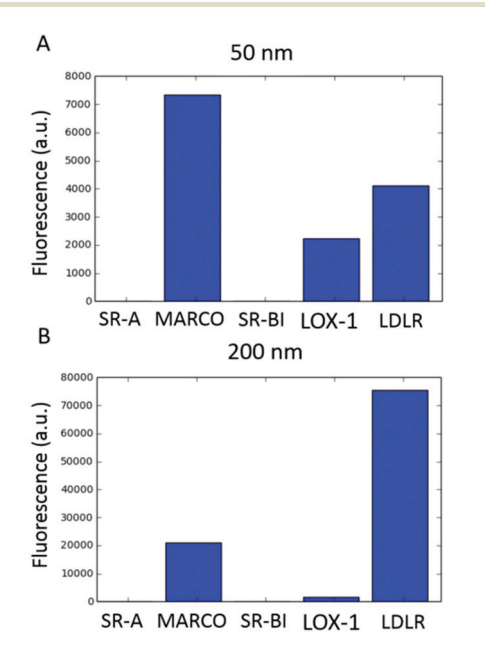


Fig. 3 Putative scavenger uptake pathways of silica nanoparticles into A549 cells extracted from mathematical analysis. (A) 50 nm and (B) 200 nm silica nanoparticles

that show almost no uptake when dispersed in 30% foetal bovine serum, as previously observed. 18,26 The reduction of uptake in the presence of higher concentrations of protein was, furthermore, observed both for foetal bovine and human serum, again as observed previously.26

Though the nanoparticles were taken up less in higher concentrations of serum, pre-incubation with scavenger receptor inhibitor (poly I) reduces uptake further, compared to the absence of inhibitor (Fig. S6†). Subsequently, nanoparticle uptake in high serum concentrations in cells silenced for scavenger receptors was investigated. Uptake of 10 nm nanoparticles showed similar behaviour upon silencing specific scavenger receptors when the nanoparticles were dispersed in 30% and 50% foetal bovine serum (Fig. 4A and D) compared to under normal cell culture conditions (10% foetal bovine serum; Fig. 1B). Similarly, the 50 nm silica nanoparticles showed high uptake in LOX-1 silenced cells in both 30% and 50% foetal bovine serum (Fig. 4B and E), as in lower serum amounts (10% foetal bovine serum; Fig. 1C). The 200 nm nanoparticles, on the other hand, have a very low uptake when dispersed in 30% and 50% foetal bovine serum and therefore no difference in uptake among silenced cells could be observed.

Experimental

Materials and methods

Nanoparticle preparation and characterization. Silica nanoparticles with an arginine shell were kindly provided by Dr Eugene Mahon prepared as previously described.²¹ The nanoparticles were dispersed in the relevant media prior to measurement of their hydrodynamic diameter and zeta potential on a Malvern Nanosizer ZS. Size measurements were averaged over 3 × 11 runs at 25 °C, while zeta potential experiments were averaged over two runs of between 10 and 100 scans at 25 °C.

Human serum. To prepare human serum (HS) for this study, blood samples were collected from approximately 10 different volunteers under approval from the Human Research Ethics committee at University College Dublin, Ireland. Clot activator was added to the blood, after which it was incubated at room temperature for 45 min and centrifuged for 15 min at 2000 RCF. The supernatant (serum) was collected and preserved in cryovials at -80 °C. Before performing an experiment the serum was allowed to thaw on ice.

Cell culture. Tissue culture reagents were purchased from GIBCO Invitrogen Corporation/Life Technologies Life Sciences (Carlsbad, CA) unless otherwise specified. Fucoidan, polyinosinic acid (poly I) and polycytidylic acid (poly C) were purchased from Sigma-Aldrich (Ireland). A549 cells (ATCC-CCL-185) were maintained as monolayer cultures in MEM supplemented with 10% foetal bovine serum (cMEM) at 37 °C and 5% CO₂.

Blocking of scavenger receptors with inhibitors. A549 cells (80 000 cells) were seeded onto 24 well plates (Greiner Bio-One, UK) and incubated for 24 h. Subsequently, the medium was

Paper

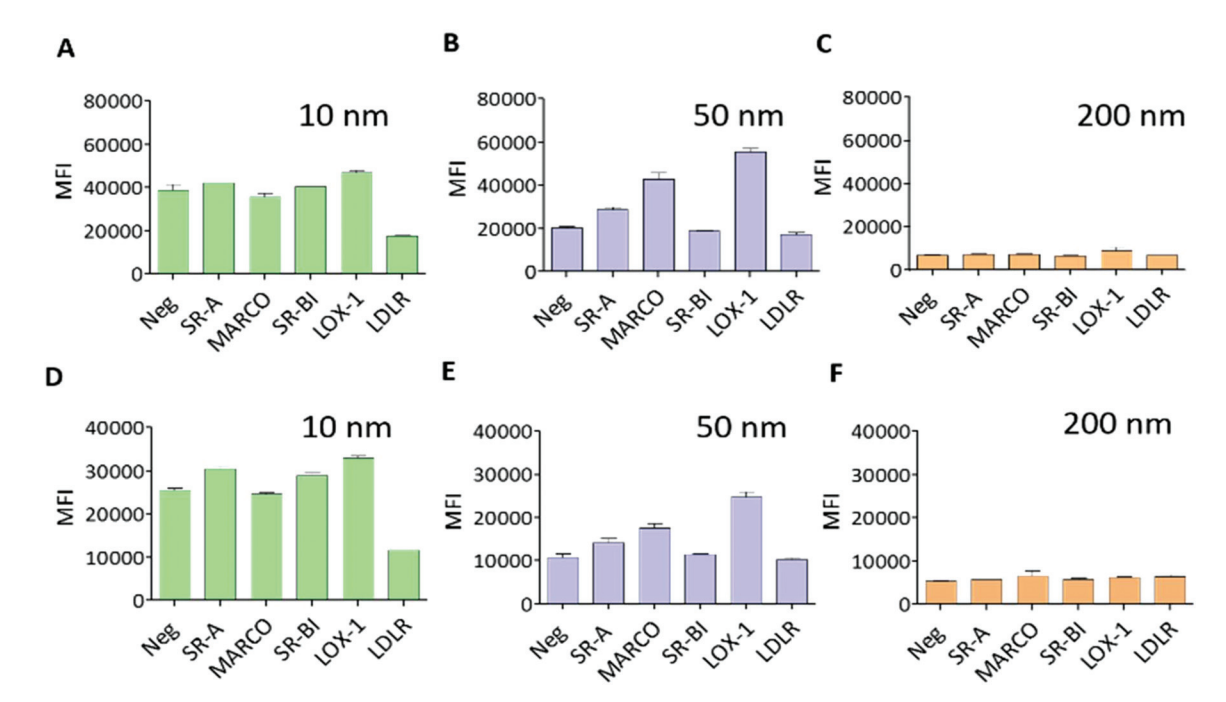


Fig. 4 Effect of the concentration serum in cellular uptake of silica nanoparticles in A549 cells. Nanoparticle uptake in A549 cells silenced for the scavenger receptors SR-A, MARCO, SR-BI, LOX-1 and LDLR or negative silencer control (Neg). Cells were silenced for 72 h before exposure for 3 h to $100 \mu g \text{ mL}^{-1}$ of (A, D) 10 nm, (B, E) 50 nm and (C, F) 200 nm silica nanoparticles dispersed in 30% (A, B, C) or 50% (D, E, F) foetal bovine serum. Results are presented as the median cell fluorescence intensity (MFI) due to nanoparticle uptake.

removed, the cells were washed with serum free MEM and the cells incubated with either poly I, poly C or fucoidan at different concentrations for 30 min. Next, the inhibitor solution was removed and a suspension of 100 $\mu g\ ml^{-1}$ nanoparticles in cMEM added to the cells. The cells were incubated with the nanoparticles for 3 h, after which they were analysed by flow cytometry.

Real-time polymerase chain reaction (qPCR). RNAs were extracted by Invitrap Spin Cell RNA mini kit (STRATEC Molecular, Germany). The RNA was then reversed transcribed to cDNA by High Capacity cDNA Reverse Transcription Kit (Applied Biosystems, Ireland). The mRNA levels were measured by real time PCR (ABI PRISM 7700 detection system, Applied Biosystems, Ireland) using Power SYBR® Green PCR Master Mix (Applied Biosystems, Ireland). Silencer Select siRNA (Ambion, Ireland) was used for silencing scavenger receptors in A549 cells. Two siRNAs (Table S1†) were used to knockdown expression of each scavenger receptor in order to compare the efficiency of gene silencing.

Cell silencing and flow cytometry. A549 cells (13 000 cells) were seeded onto 24 well plates (Greiner Bio-One, UK), and incubated for 24 h prior to silencing of the gene coding for SR-A, SR-BI, MARCO, LOX-1 or LDLR. Next, the cells were transfected with 30 pmol of Silencer Select siRNA (Ambion, Ireland) using Oligofectamine (Invitrogen, Ireland) according to the manufacturer's instructions. Neg1 silencer was used as a negative control. Cells were transfected with siRNAs for 72 h prior to exposure to nanoparticles in all experiments.

In order to expose the cells to the nanoparticles, cells were washed for 10 min in serum free MEM. The medium was then replaced by the nanoparticle dispersions and incubated further. All nanoparticle dispersions were freshly prepared by diluting the nanoparticle stock in different concentration of serum-containing MEM.

To prepare the samples for flow cytometry, the cells were washed 3 times with DPBS and harvested with trypsin/EDTA. Cell pellets were then fixed at room temperature with 4% formalin solution neutral buffered (Sigma, Ireland) for 20 min and re-suspended with constant volumes of DPBS before cell-associated fluorescence (15 000 cells per sample) was detected using an Accuri C6 reader (BD Accuri Cytometers Inc., Ireland). The results are reported as the median of the distribution of cell fluorescence intensity, averaged over 2 independent replicas; error bars represent the standard deviation between replicas.

Conclusions

In this work, we report evidence of reciprocal up and down regulation of other scavenger receptors after knock-down of a specific scavenger receptor in A549 lung epithelial cells. This indicates overlapping role of these receptors and complicates the interpretation of experiments where silencing a receptor is used to identify the role of that receptor in uptake of, in our case, nanoparticles. Exposing cells to 10, 50 and 200 nm silica nanoparticles, we show that the 50 and 200 nm silica nano-

Nanoscale Paper

particles are taken up by scavenger receptors also in these non-phagocytic cells, similarly to previous reports for phagocytic cells. 16

The reciprocal up and down regulation of scavenger receptors leads to complex behaviour when studying uptake of the silica nanoparticles in silenced cells. For example, knock-down of the LOX-1 receptor does not lead to a decreased uptake but rather a higher uptake of both the 50 and 200 nm silica nanoparticles. Knowing that the MARCO scavenger receptor is substantially up-regulated under these conditions suggests that MARCO mediates uptake of these nanoparticles, but this interpretation can only be made with access to the expression levels of the other receptors. We illustrate the idea behind such considerations using a mathematical model that uses the expression levels to disentangle the pathways. The results show an involvement of the MARCO and LDLR receptors in the uptake of the 50 and 200 nm silica nanoparticles, but we should stress that the procedure is mainly illustrative. That is, the higher uptake could potentially also be due to upregulation of other receptors not included in this study. We did not attempt to investigate all such potential co-regulators systematically. Future studies need to confirm these conclusions with alternative methodology, for example overexpression of the relevant receptors.²³

Increasing the serum concentration of the medium the nanoparticles are dispersed in towards more realistic concentrations reduces uptake rate, as previously observed. However, the involvement of scavenger receptors in the uptake remains.

This study sheds light on the importance of scavenger receptors in the uptake of nanoparticles by non-phagocytic cells, but more generally highlights complications when using RNA interference to study nanoparticle cellular uptake. Since many biological systems have strong links between receptors, uptake experiments could easily be misinterpreted in the absence of a thorough and systematic investigation.

Conflicts of interest

There are no conflicts of interest to declare.

Acknowledgements

The authors would like to thank Dr Eugene Mahon for kindly providing the nanoparticles for this study. KP was supported by the Irish Research Council (IRC) through an EMPOWER Postdoctoral Fellowship Scheme, and was partially supported by the Faculty of Science, Mahidol University, and by Thailand Research Fund. RM was supported by UCD CSC Scholarship Scheme 2012. CÅ was partially supported by Science Foundation Ireland (09/RFP/MTR2425) and the European Union Seventh Framework Programme project NanoTransKinetics (grant 266737). agreement Additionally, the results presented are based on work supported by the EU FP7 Capacities project QualityNano (grant no. INFRA-2010-262163).

References

- 1 K. Park, ACS Nano, 2013, 7, 7442-7447.
- 2 W. R. Sanhai, J. H. Sakamoto, R. Canady and M. Ferrari, Nat. Nanotechnol., 2008, 3, 242-244.
- 3 N. Oh and J.-H. Park, Int. J. Nanomed., 2014, 9, 51-63.
- 4 H. H. Gustafson, D. Holt-Casper, D. W. Grainger and H. Ghandehari, *Nano Today*, 2015, **10**, 487–510.
- 5 A. Lesniak, A. Salvati, M. J. Santos-Martinez, M. W. Radomski, K. A. Dawson and C. Åberg, J. Am. Chem. Soc., 2013, 135, 1438–1444.
- 6 J. E. Murphy, P. R. Tedbury, S. Homer-Vanniasinkam, J. H. Walker and S. Ponnambalam, *Atherosclerosis*, 2005, 182, 1–15.
- 7 R. F. Hamilton, S. A. Thakur, J. K. Mayfair and A. Holian, J. Biol. Chem., 2006, 281, 34218–34226.
- 8 Y. Chao, M. Makale, P. P. Karmali, Y. Sharikov, I. Tsigelny, S. Merkulov, S. Kesari, W. Wrasidlo, E. Ruoslahti and D. Simberg, *Bioconjugate Chem.*, 2012, 23, 1003–1009.
- 9 Y. Chao, P. P. Karmali, R. Mukthavaram, S. Kesari, V. L. Kouznetsova, I. F. Tsigelny and D. Simberg, ACS Nano, 2013, 7, 4289–4298.
- 10 J. H. Shannahan, R. Podila, A. A. Aldossari, H. Emerson, B. A. Powell, P. C. Ke, A. M. Rao and J. M. Brown, *Toxicol. Sci.*, 2015, 143, 136–146.
- 11 A. Lesniak, F. Fenaroli, M. P. Monopoli, C. Åberg, K. A. Dawson and A. Salvati, *ACS Nano*, 2012, **6**, 5845–5857.
- 12 R. Foldbjerg, J. Wang, C. Beer, K. Thorsen, D. S. Sutherland and H. Autrup, *Chem.-Biol. Interact.*, 2013, **204**, 28–38.
- 13 J. Kasper, M. Hermanns, C. Bantz, O. Koshkina, T. Lang, M. Maskos, C. Pohl, R. Unger and C. J. Kirkpatrick, *Arch. Toxicol.*, 2013, 87, 1053–1065.
- 14 S. Vranic, I. Garcia-Verdugo, C. Darnis, J.-M. Sallenave, N. Boggetto, F. Marano, S. Boland and A. Baeza-Squiban, Environ. Sci. Pollut. Res., 2013, 20, 2761–2770.
- 15 R. Iyer, R. F. Hamilton, L. Li and A. Holian, *Toxicol. Appl. Pharmacol.*, 1996, 141, 84–92.
- 16 G. A. Orr, W. B. Chrisler, K. J. Cassens, R. Tan, B. J. Tarasevich, L. M. Markillie, R. C. Zangar and B. D. Thrall, *Nanotoxicology*, 2011, 5, 296–311.
- 17 R. Biswas, R. F. Hamilton and A. Holian, *J. Immunol. Res.*, 2014, 2014, 10.
- 18 A. Salvati, A. S. Pitek, M. P. Monopoli, K. Prapainop, F. Baldelli Bombelli, D. R. Hristov, P. M. Kelly, C. Åberg, E. Mahon and K. A. Dawson, *Nat. Nanotechnol.*, 2013, 8, 137–143.
- 19 K. Zarschler, K. Prapainop, E. Mahon, L. Rocks, M. Bramini, P. M. Kelly, H. Stephan and K. A. Dawson, *Nanoscale*, 2014, 6, 6046–6056.
- 20 A. Dieudonné, D. Torres, S. Blanchard, S. Taront, P. Jeannin, Y. Delneste, M. Pichavant, F. Trottein and P. Gosset, *PLoS One*, 2012, 7, e41952.

Paper Nanoscale

- 21 E. Mahon, D. R. Hristov and K. A. Dawson, Chem. Commun., 2012, 48, 7970-7972.
- 22 K. Shapero, F. Fenaroli, I. Lynch, D. C. Cottell, A. Salvati and K. A. Dawson, Mol. BioSyst., 2011, 7, 371-378.
- 23 S. Lara, F. Alnasser, E. Polo, D. Garry, M. C. Lo Giudice, D. R. Hristov, L. Rocks, A. Salvati, Y. Yan and K. A. Dawson, ACS Nano, 2017, 11, 1884-1893.
- 24 P. I. Mäkinen, J. P. Lappalainen, S. E. Heinonen, P. Leppänen, M. T. Lähteenvuo, J. V. Aarnio, J. Heikkilä, M. P. Turunen and S. Ylä-Herttuala, Cardiovasc. Res., 2010, 88, 530-538.
- 25 J. A. Kim, C. Åberg, A. Salvati and K. A. Dawson, Nat. Nanotechnol., 2012, 7, 62-68.
- 26 J. A. Kim, A. Salvati, C. Åberg and K. A. Dawson, Nanoscale, 2014, 6, 14180-14184.

AAPS PharmSciTech

The impact of serum proteins and surface chemistry on magnetic nanoparticle colloidal stability and cellular uptake in breast cancer cells --Manuscript Draft--

Manuscript Number:	
Full Title:	The impact of serum proteins and surface chemistry on magnetic nanoparticle colloidal stability and cellular uptake in breast cancer cells
Article Type:	Research Article
Section/Category:	NOT APPLICABLE (Choose this section if you have NOT been invited to submit a manuscript)
Keywords:	superparamagnetic iron oxide nanoparticles; biological media; colloidal stability; cancer cell
Corresponding Author:	Kanlaya Prapainop, D.Phil Faculty of Science, Mahidol University Ratchatewi, Bangkok THAILAND
Corresponding Author Secondary Information:	
Corresponding Author's Institution:	Faculty of Science, Mahidol University
Corresponding Author's Secondary Institution:	
First Author:	Wid Mekseriwattana
First Author Secondary Information:	
Order of Authors:	Wid Mekseriwattana
	Supreeya Srisuk
	Ruttanaporn Kriangsaksri
	Nuttawee Niamsiri
	Kanlaya Prapainop, D.Phil
Order of Authors Secondary Information:	
Manuscript Region of Origin:	THAILAND
Abstract:	Superparamagnetic iron oxide nanoparticles (SPIONs) have been extensively studied in biomedical applications for therapeutic or diagnostic purposes. Stability is one of the key determinants dictating successful application of these nanoparticles (NPs) in biological systems. In this study, SPIONs were synthesized and coated with two protective shells: poly(methacrylic acid) (PMAA) or citric acid (CA) and the stability was evaluated in biologically relevant media together with effect of serum protein supplementation. The stabilities of SPION, SPION-PMAA and SPION-CA in water, DMEM, RPMI, DMEM with 10% (v v-1) and RPMI with 10% (v v-1) fetal bovine serum were determined. Without protective shells, the NPs were not stable and formed large aggregates in all media tested. CA improved the stability of the NPs in water, but was not very effective in improving stability in cell culture media. Addition of serum slightly improved colloidal stability of SPION-CA, whereas inclusion of serum significantly improved the colloidal stability of SPION-PMAA. Serum proteins also found to enhance cellular viability of MCF-7 breast cancer cells after exposure to high concentrations of SPION-PMAA and SPION-CA. Different patterns of serum proteins binding to the NPs were observed and cellular uptake in MCF-7 cells were investigated. The stabilized SPION-PMAA and SPION-CA NPs showed uptake activity with minimal background attachment. Therefore, the importance of colloidal stability of SPIONs for utilizing in future therapeutic or diagnostic purposes is illustrated.
Suggested Reviewers:	António José Ribeiro University of Coimbra

Opposed Reviewers:	Ping Yang University of Jinan mse_yangp@ujn.edu.cn Expertise in the field
	Khalid M. El-Say King Abdulaziz University kelsay1@kau.edu.sa
	Mikio Kakumoto Ritsumeikan University mickeyka@fc.ritsumei.ac.jp Expertise in the field
	aribeiro@ff.uc.pt Expertise in the field



Dr. Kanlaya Prapainop Department of Biochemistry, Faculty of Science, Mahidol University Bangkok, Thailand Tel: +66 2 201 5604

Email: Kanlaya.pra@mahidol.edu

26th October 2018

Dear Editor of An Official Journal of the American Association of Pharmaceutical Scientists,

I am pleased to submit an original research article entitled "The impact of serum proteins and surface chemistry on magnetic nanoparticle colloidal stability and cellular uptake in breast cancer cells" by Wid Mekseriwattana, Supreeya Srisuk, Ruttanaporn Kriangsaksri, Nuttawee Niamsiri and Kanlaya Prapainop for consideration for publication in AAPS PharmSciTech.

In this manuscript, we compared stability of superparamagnetic iron oxide nanoparticles (SPIONs) and SPIONs with two different surface coating poly(methacrylic acid) (PMAA) and citric acid (CA) in different biological medium. It has been shown that without any surface coating, the particles were severely unstable and formed large aggregates in all conditions. However the PMAA and CA could improve the colloidal stability of the particles in water. In particular, PMAA is more effective in improving the SPION stability under cell culture medium conditions. Addition of fetal bovine serum was also improve the stability of particles. The effect of those biological conditions not only be found to impact on behavior of the particles in suspension but also impact to cellular uptake in breast cancer cells. In addition, different proteins were found to bind each particles differently and it might contribute to the different cellular response. Therefore this manuscript addresses an important area of interaction of SPIONs and different surface coated SPIONs with relevant biological environment that the particles are exposed to. These finding can bring some inside in understanding how various surface coated nanoparticles behave in term of colloidal stability, serum protein binding, and cellular uptake which could lead to further understanding or better design particles for drug delivery and imaging for treatment and diagnosis of various diseases. We believe that this manuscript appropriate for publication by AAPS PharmSciTech because it has interdisciplinary studies involved in materials science, biochemistry studies and cell biology.

This manuscript has 4,111 words with 6 figures and is now not under consideration for publication elsewhere. We have no conflicts of interest to disclose.

Thank you for your kind consideration.

Sincerely,



Kanlaya Prapainop Lecturer, Department of Biochemistry, And School of material science and innovation, Faculty of Science, Mahidol University Title Page

The impact of serum proteins and surface chemistry on magnetic

nanoparticle colloidal stability and cellular uptake in breast cancer cells

Wid Mekseriwattana¹, Supreeya Srisuk², Ruttanaporn Kriangsaksri², Nuttawee

Niamsiri³ and Kanlaya Prapainop*, 1, 2

¹ School of Materials Science and Innovation, Faculty of Science, Mahidol University, Bangkok, Thailand

²Department of Biochemistry, Faculty of Science, Mahidol University, Bangkok, Thailand

³ Department of Biotechnology, Faculty of Science, Mahidol University, Bangkok, Thailand

Email address: kanlaya.pra@mahidol.edu

Postal address: 272 Rama VI Road, Ratchathewi district, Bangkok 10400, Thailand

Office number:

suggested running head: magnetic nanoparticle colloidal stability

1 2

3

4

5

6

7 8

9

10

11

12

13

14

15 16

17

18

Abstract. Superparamagnetic iron oxide nanoparticles (SPIONs) have been extensively studied in biomedical applications for therapeutic or diagnostic purposes. Stability is one of the key determinants dictating successful application of these nanoparticles (NPs) in biological systems. In this study, SPIONs were synthesized and coated with two protective shells: poly(methacrylic acid) (PMAA) or citric acid (CA) and the stability was evaluated in biologically relevant media together with effect of serum protein supplementation. The stabilities of SPION, SPION-PMAA and SPION-CA in water, DMEM, RPMI, DMEM with 10% (v v⁻¹) and RPMI with 10% (v v⁻¹) fetal bovine serum were determined. Without protective shells, the NPs were not stable and formed large aggregates in all media tested. CA improved the stability of the NPs in water, but was not very effective in improving stability in cell culture media. Addition of serum slightly improved colloidal stability of SPION-CA, whereas inclusion of serum significantly improved the colloidal stability of SPION-PMAA. Serum proteins also found to enhance cellular viability of MCF-7 breast cancer cells after exposure to high concentrations of SPION-PMAA and SPION-CA. Different patterns of serum proteins binding to the NPs were observed and cellular uptake in MCF-7 cells were investigated. The stabilized SPION-PMAA and SPION-CA NPs showed uptake activity with minimal background attachment. Therefore, the importance of colloidal stability of SPIONs for utilizing in future therapeutic or diagnostic purposes is illustrated.

Keywords: superparamagnetic iron oxide nanoparticle, biological media, colloidal stability, cancer cell

Introduction

Superparamagnetic iron oxide nanoparticles (SPIONs) have shown great potential in biomedical applications both *in vitro* and *in vivo* for therapeutic or diagnostic purposes such as cell labelling, biological separation and tracking (1-4). In general, SPIONs are coated with protective shells such as polymers, silica, or surfactants (5-8). Surface coating is an important component of the SPIONs as it enhances their stability by protecting the nanoparticles (NPs) from agglomeration and oxidation from the environment. Additionally, coatings could provide available surface functionalities for further modification with other desirable ligands, increase the biocompatibility, and reduce reticuloendothelial system (RES) elimination while increasing nanoparticle uptake by specific cells (5, 7, 9). It has been shown that surface modifications lead to different surface properties and cellular responses to the NPs. NPs with negative surface charges usually exhibit lower cytotoxicity and have less non-specific uptake than positively-charged NPs. Thus, the negatively charged surface is more compatible for use in cellular studies (10, 11). Poly(methacrylic acid) (PMAA) and citric acid (CA) are anionic coatings that we focused on in this study because these coatings are able to increase SPIONs stability in aqueous systems (6, 12).

Another requirement for the effective use of NPs in biological applications is stability under physiological conditions. Proteins in biological media could be absorbed on the NPs and alter their stability, potentially resulting in different cellular behaviour and cytotoxicity from the original forms of the NPs (13-18). Despite the importance of the impact biological media has on NP activity, *in vitro* and *in vivo* studies characterizing CA and PMAA surface coatings on SPIONs in physiological environments is limited. Thus, in this study, SPIONs coated with negatively-charged poly(methacrylic acid) (SPION-PMAA) and citric acid (SPION-CA) are investigated for stability in biological media with and without the presence of serum proteins, and for differences in the cellular uptake responses in breast cancer cells. This study will provide important information for better understanding the influence of surface coatings on the NP stability and activity, which will allow for improved design of SPIONs for *in vivo* applications.

Materials and methods

Materials

Ferrous chloride tetrahydrate (FeCl₂·4H₂O), ferric chloride hexahydrate (FeCl₃·6H₂O), methacrylic acid (MAA), sodium dodecyl sulfate (SDS), potassium persulfate (K₂S₂O₈), neutral red, potassium hexacyanoferride, sodium thiosulfate and sodium carbonate were obtained from Sigma-Aldrich. Ammonia solution (NH₄OH, 25%) and tri-sodium citrate dihydrate were obtained from Merck.

Hydrochloric acid was obtained from Riedel-de Haen. Silver nitrate was obtained from RCI Labscan. EDTA disodium salt dihydrate was obtained from Vivantis. 3-(4,5-Dimethyl-2-thiazolyl)-2,5-diphenyl-2H-tetrazolium bromide (MTT) was obtained from PanReac AppliChem. Dulbecco's Modified Eagle's Medium (DMEM), Roswell Park Memorial Institute's medium (RPMI), fetal bovine serum (FBS) and Penicillin/Streptomycin (P/S) were obtained from Gibco. Bovine serum albumin (BSA) was obtained from Capricorn Scientific. Dimethyl sulfoxide (DMSO) was obtained from Fisher Scientific. Sodium chloride, potassium chloride, di-sodium hydrogen phosphate dihydrate and potassium dihydrogen phosphate were obtained from VWR Chemicals. All chemicals were used as purchased without further purification.

Synthesis of SPIONs

SPIONs were synthesized by a co-precipitation method modified from Petcharoen and Sirivat (19). In brief, FeCl₂·4H₂O (0.75 g) and FeCl₃·6H₂O (2.5 g) were dissolved in 45 mL water. The mixture was heated to 80 °C with vigorous stirring under N_2 atmosphere. NH₄OH (25%, 5 mL) was added to the solution which rapidly changed the color to black. The reaction was maintained at this temperature for 10 minutes. The NPs were washed several times with water by magnetic decantation and dispersed in water as stock solution.

Synthesis of SPION-PMAA

The coating process was performed using a protocol modified from that reported by Yu and Chow (20). SPION stock solution (10 mL) was dispersed in 200 mL water. SDS (1.15 g) was added, and the solution was stirred and heated to 70 °C followed by addition of 1 mL of neat MAA. After 45 minutes, $K_2S_2O_8$ solution (0.13 g mL⁻¹, 15 mL) was added, and the solution was further stirred for 2 hours. The NPs were washed several times with water to remove excess coating agents and then separated by magnetic decantation and dried in an oven for subsequent characterization.

Synthesis of SPION-CA

The citrate coated SPIONs were synthesized following the method reported by Nigam et al. (21). Briefly, FeCl₂·4H₂O (3.7 g) and FeCl₃·6H₂O (0.87 g) were dissolved in 40 mL water and refluxed at 70 °C under N₂ atmosphere with vigorous stirring for 30 minutes. NH₄OH (25%, 10 mL) was added and the reaction was maintained at this temperature for another 30 minutes. Tri-sodium citrate dihydrate solution (0.75 g mL⁻¹, 2 mL) was added and the temperature was raised to 90 °C for 1 hour. The resulting SPION-CA were washed with water and separated by magnetic decantation and then dispersed in water as stock solution.

Preparation of SPIONs corona

Stock solutions of SPION, SPION-PMAA and SPION-CA were dispersed in DMEM with 10% FBS to final concentration of 0.2 mg mL⁻¹ and incubated at room temperature for 24 hours. The coronas were separated using centrifugation for further experiments.

Nanoparticle characterization

Functional groups and surface coatings of the particles were studied by infrared spectrometry (Perkin Elmer Frontier FTIR spectrometer and Bruker ALPHA FTIR spectrometer). Hydrodynamic size and zeta potential were analyzed using a Nanosizer 90 ZS (Malvern Instrument, UK). The particle size and morphology were analyzed using a transmission electron microscope (FEI Tecnai T20, USA).

Stability evaluation of the magnetic colloidal suspension

SPION, SPION-PMAA, SPION-CA were suspended in water, phosphate buffered saline (PBS), DMEM, DMEM with 10% FBS, RPMI or RPMI with 10% FBS. Size and zeta potential were measured at different times of incubation using a Zetasizer Nano-ZS90 to determine the stability of the particles in each medium.

Effect of SPION, SPION-PMAA and SPION-CA on MCF-7 cells viability

MCF-7 cells were cultured in DMEM medium supplemented with 10% of FBS and 1% P/S. Cells were maintained at 37 °C with 5% CO₂ in a humidified incubator. The cells were seeded onto a 96-well plate with a cell density of 8 x 10^3 cells per well and incubated for 24 hours. Different concentrations of SPION, SPION-PMAA and SPION-CA were mixed with DMEM in the presence or absence of FBS and added to the cells. After 6 and 24 hours of treatment, the media was removed. The cells were washed with PBS then $100 \,\mu$ L of MTT solution (0.5 mg mL⁻¹ in DMEM medium) was added and incubated for 3 hours at 37 °C under 5% CO₂ in a humidified incubator. After incubation, the media was removed and $100 \,\mu$ L of DMSO was added to each well. Cell viability was determined by measuring the absorbance at 540 nm using a microplate reader (Tecan Spark 10M).

Cellular uptake

MCF-7 cells were cultured in DMEM medium supplemented with 10% of FBS and 1% P/S. Cells were maintained at 37 °C with 5% CO₂ in a humidified incubator. The cells were seeded onto a 24-well plate containing circular coverslips with a cell density of 1 x 10⁵ cells per well and incubated for 24 hours. The medium was discarded and replaced with fresh medium containing 50 μg mL⁻¹ of either SPION, SPION-PMAA or SPION-CA. After 24 hours of incubation, the cells were washed once with DMEM medium followed by 3 washes with PBS, and fixed with 3.6% paraformaldehyde. The cells were immersed in 2% ferrocyanide/2% HCl solution for iron staining followed by counter staining in

0.5% neutral red solution. NPs uptake was observed under an optical microscope (Nikon Eclipse T E2000-U).

Results

115

116

117

118

119

120

Nanoparticle characterization

The size and morphology of the SPION, SPION-PMAA and SPION-CA particles were observed by TEM as shown in figure 1. The TEM images showed that uncoated SPION had an irregular

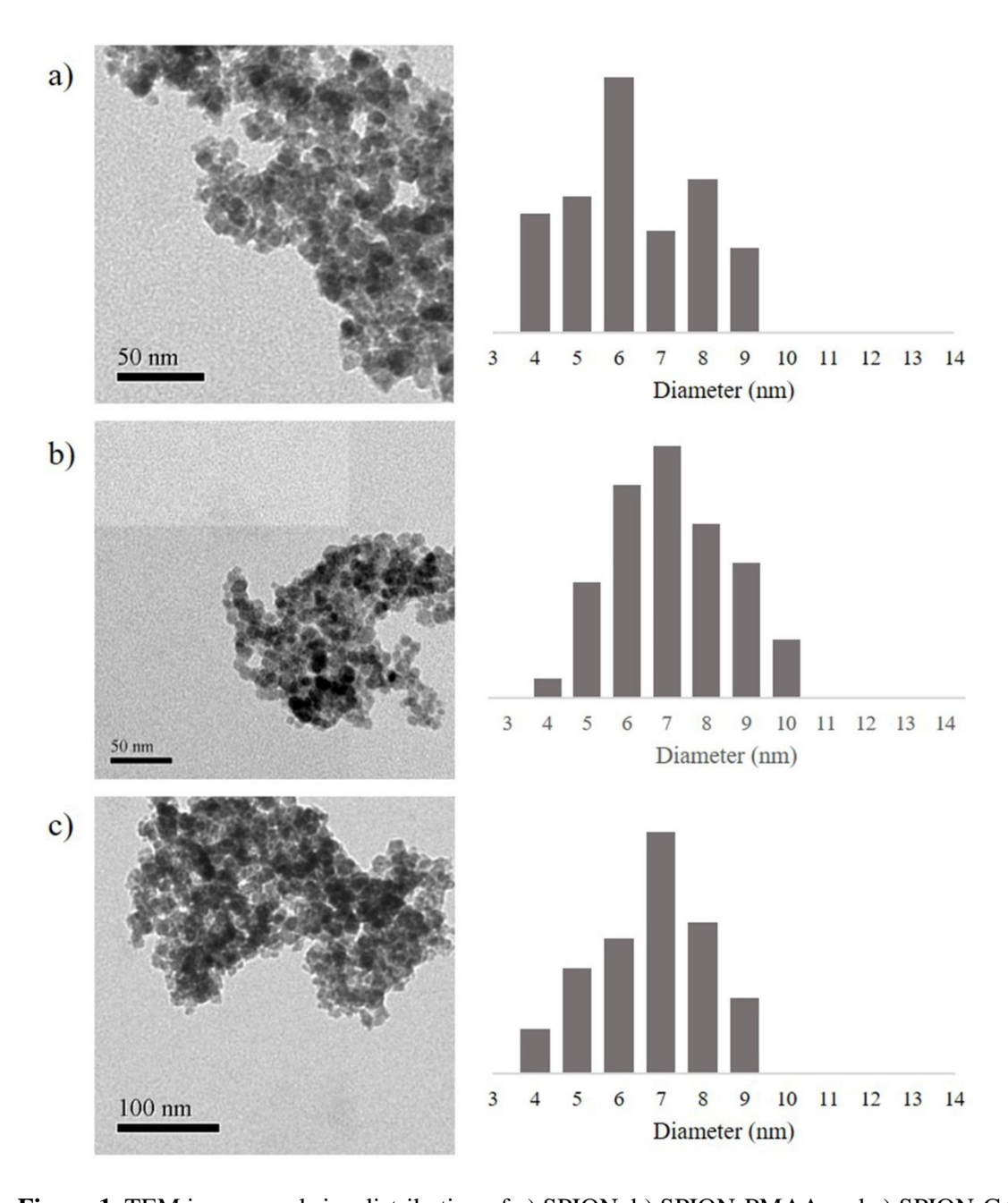


Figure 1. TEM images and size distribution of a) SPION, b) SPION-PMAA and c) SPION-CA.

shape with a diameter of around 6 nm. Surface coating with PMAA or CA did not significantly increase the size, but promoted a more spherical morphology with a smoother surface compared to the uncoated SPION.

FTIR spectra were recorded to confirm NP surface modification as shown in figure 2a. The peaks around 540 cm⁻¹ observed in all three samples represent the vibration of Fe-O bonds which is a characteristic peak of iron oxide. Hydroxyl groups on the nanoparticle surface are evidenced by the stretching vibrational peaks at around 1620 and 3200 cm⁻¹. The coating of PMAA on the SPION was confirmed by the observation of C-H stretching peaks at 2855 and 2924 cm⁻¹. The peak which appeared at 1400 cm⁻¹ can be attributed to symmetrical stretching of a C=O bond, suggesting symmetric binding between the polymer and the nanoparticle surface. SPION-CA showed peaks at 1406 and 1580 cm⁻¹ which correspond to the symmetric stretch of COO⁻ and vibration of C=O from citrate molecules.

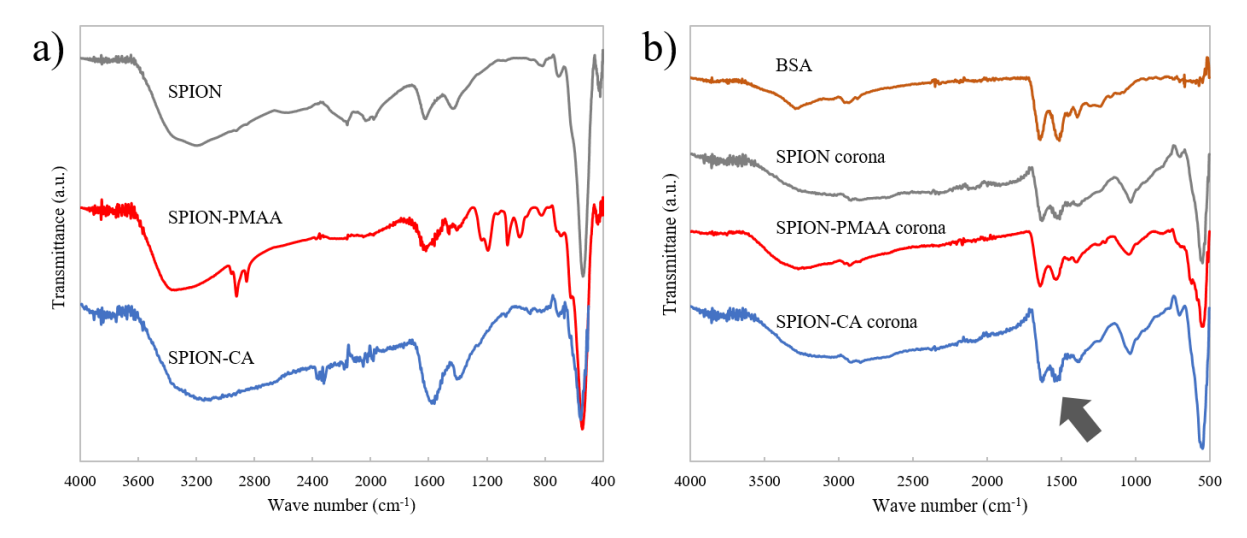


Figure 2. a) FTIR spectra of SPION, SPION-PMAA and SPION-CA. b) FTIR spectra of BSA and coronas of SPION, SPION-PMAA and SPION-CA.

Stability evaluation of the magnetic colloidal suspension

SPION, SPION-PMAA and SPION-CA were suspended in commonly used biological media: water, PBS, DMEM, DMEM with 10% FBS, RPMI and RPMI with 10% FBS and the colloidal stability was evaluated by determination of the hydrodynamic size using dynamic light scattering (figure 3). The uncoated SPION showed rapid aggregation in water, giving a diameter of >1 μ m (figure 3a). Surface modification of SPION with either PMAA or CA resulted in a smaller hydrodynamic size (~100 nm) which was maintained for at least 24 hours.

In PBS, uncoated SPION had an average diameter of \sim 500 nm, however after prolonged incubation for 24 hours, aggregation was observed resulting in an average particle diameter of size \sim 1 μ m, similar to what was observed in water. The sizes of the SPION-PMAA and SPION-CA NPs were \sim 100 nm. After 24 hours, size of SPION-CA increased to \sim 300 nm, whereas the SPION-PMAA remained the same size.

SPION and SPION-CA NPs were all highly unstable in cell culture media such as DMEM and RPMI, exhibiting aggregation with particle sizes >1 μ m (figure 3c and 3e). Upon addition of FBS to the culture media, sizes of both samples were significantly reduced. SPION-PMAA showed the highest stability with hydrodynamic size ~500 nm in DMEM but started to form aggregates after 24-hour incubation with size increased to ~1.4 μ m. Supplementation of FBS greatly improved the stability for SPION-PMAA for which the hydrodynamic size decreased from 1 μ m to ~100 nm (figure 3d and 3f).

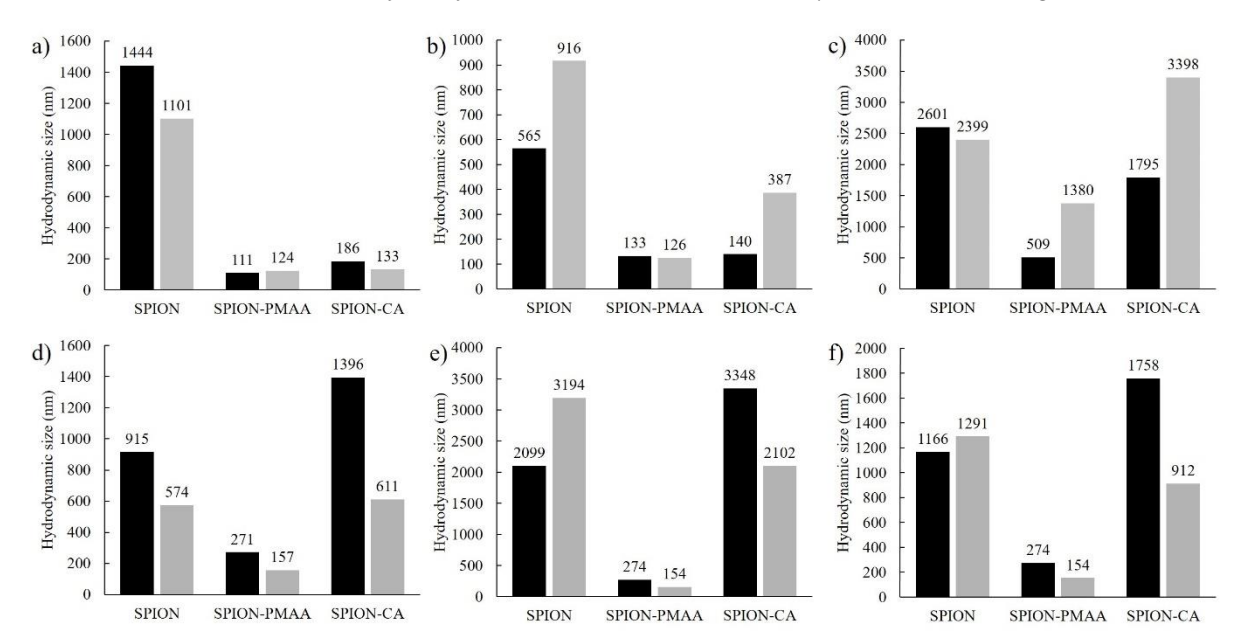


Figure 3. a)-f) Hydrodynamic size of SPION, SPION-PMAA and SPION-CA in water, PBS, DMEM, DMEM+10% FBS, RPMI and RPMI+10% FBS respectively. Black and grey bars represent 0 and 24 hours of incubation, respectively.

These size reductions in the presence of FBS could be due to the adsorption of serum proteins onto the particle, forming a protein corona on the surface which can act to prevent particle aggregation.

Formation of protein coronas were confirmed by FTIR spectroscopy (figure 2b). Coronas shows strong absorption peaks at around 1540 and 1640 cm⁻¹ matching those of BSA proteins. These peaks are attributed to vibrational modes of C=O and N-H bonds in amide linkages. SDS-polyacrylamide gel electrophoresis (SDS-PAGE) was performed to observe patterns of proteins on the NPs surface. The results show different patterns of protein bands for NPs with different coatings which could be responsible for the differences in the degree of stabilization observed among each of the NPs (figure 4).

From all the above results, among the prepared nanoparticles, SPION-PMAA had the smallest size with no changes in size even after 24 hours of incubation, indicating the best stability across the investigated media.

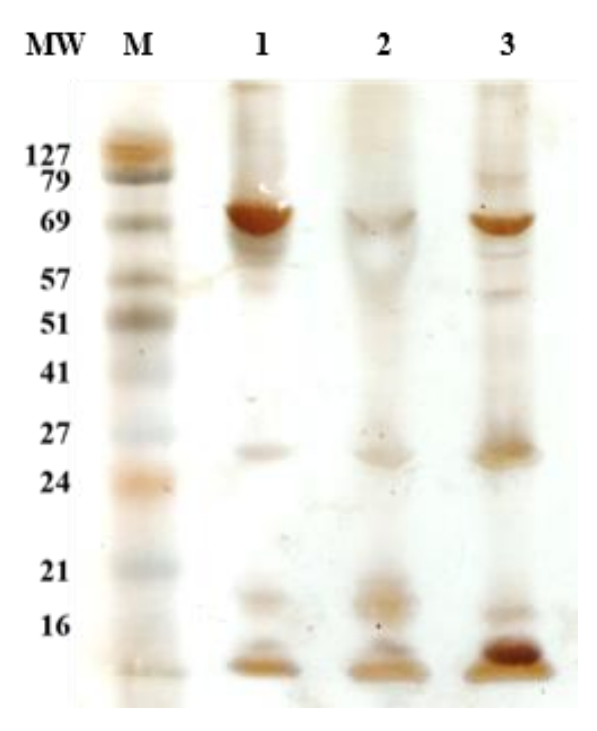


Figure 4. Protein coronas pattern observed from SDS-PAGE. Lane 1, 2 and 3 represent coronas of SPION, SPION-CA and SPION-PMAA respectively.

Effect of SPION, SPION-PMAA and SPION-CA on MCF-7 cells viability

To evaluate the potential use of the obtained magnetic NPs in cancer cells, a cellular viability assay was performed for MCF-7 breast cancer cells after NPs exposure (figure 5). With serum-free medium, the cells treated with uncoated SPION maintained nearly 100% viability, indicating the low toxicity of the NPs. In contrast, for SPION-PMAA and SPION-CA, the cell viability reduced to less than 80% when incubated for 24 hours. However, these negatively-charged SPIONs modified by PMAA or CA showed higher cellular biocompatibility than succinic anhydride-modified NPs that was previously reported with ~30% toxicity at $10~\mu g$ mL $^{-1}$ (22). Surprisingly, upon addition of FBS, the cell viability increased to over 80% for all samples. These results demonstrate that serum proteins can reduce the toxicity of the NPs towards the breast cancer cells which could be related to the formation of protein coronas on the NP surface altering the surface properties both physically and chemically.

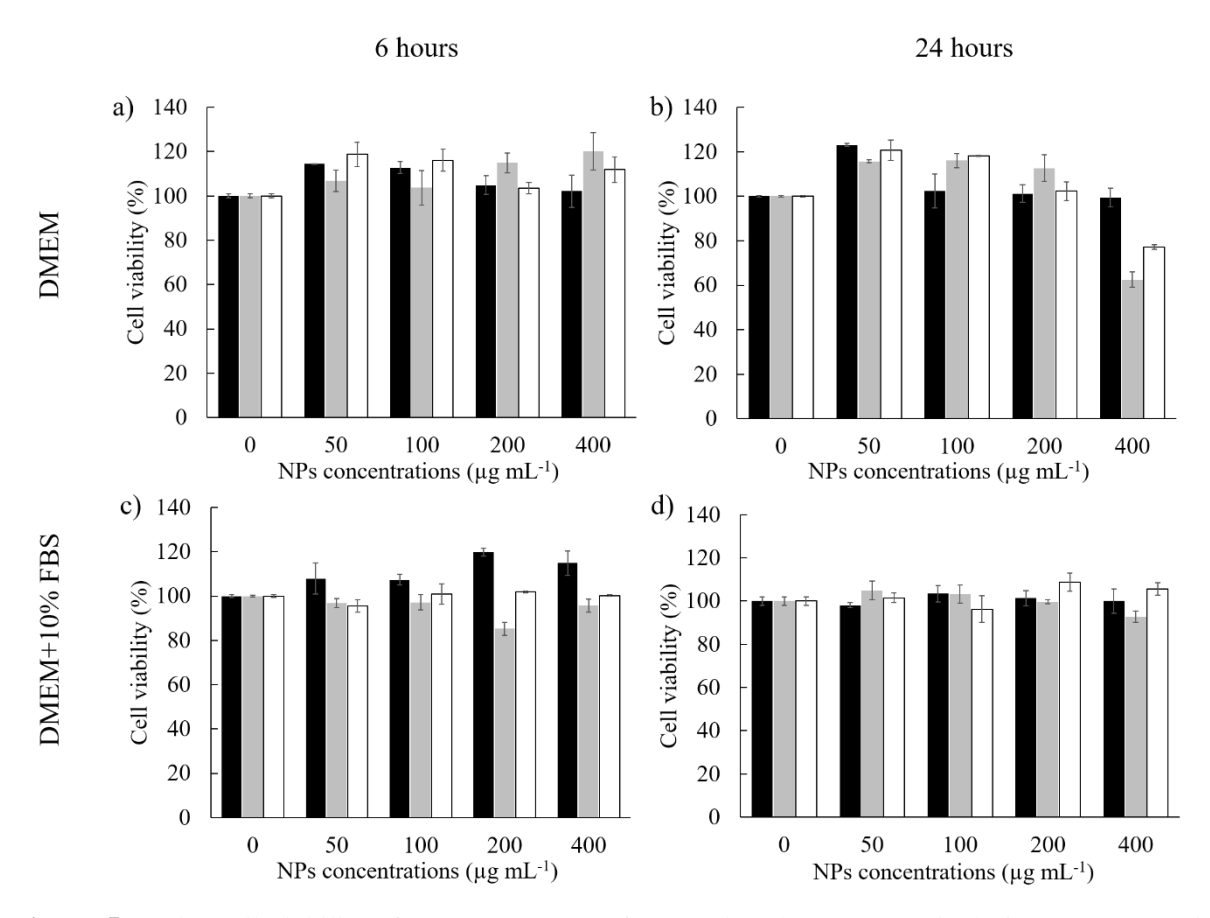


Figure 5. a), b) Cell viability after NPs treatment for 6 and 24 hours respectively in DMEM. c), d) Cell viability after NPs treatment for 6 and 24 hours respectively in DMEM+10% FBS. Black, grey and white bars represent SPION, SPION-PMAA and SPION-CA respectively.

Cellular uptake

 In order to evaluate the potential uses of the SPION in relation to its stability, cellular uptake experiments of the NPs in MCF-7 cells were performed. Significant aggregation of SPION was observed in biological media. The NPs (stained in blue color) tended to accumulate on the cells (stained in pink color) and on the coverslip surface, resulting in high non-specific background signal which interfered with cellular uptake experiments. On the other hand, SPION-PMAA, which possesses the highest stability with a size around 160 nm in complete DMEM showed a clean background with clear observation of NPs internalization into the cells. Despite the larger size of SPION-CA, the NPs shows significant higher cellular uptake when compared to SPION-PMAA. These results emphasize the importance of colloidal stability of the NPs in biomedical applications.

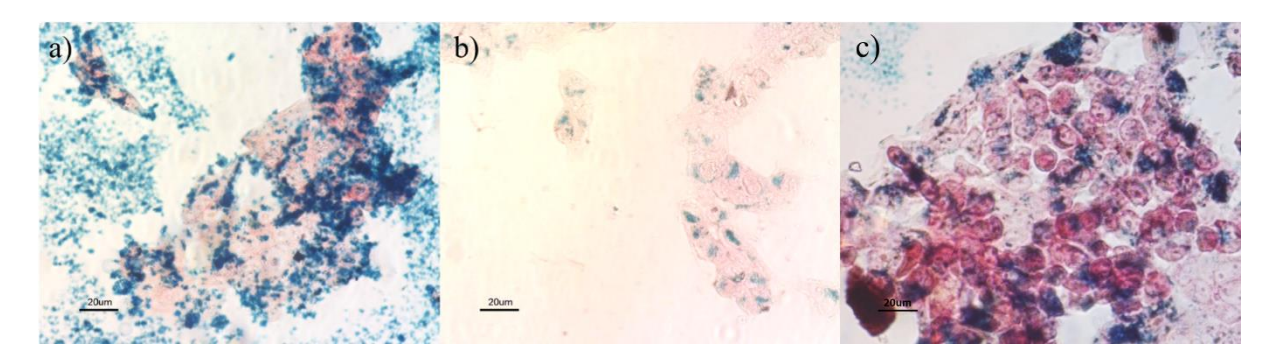


Figure 6. a)-c) Cellular uptake of SPION, SPION-PMAA and SPION-CA to MCF-7 cells respectively.

Discussion

As nanoparticles became widely explored as tools for biomedical applications, maintaining their stability in physiological environments is one of the main challenges. To maximize bioavailability, NPs are commonly modified with hydrophilic surfaces (23, 24). However, the presence of biomolecules and complex ions in biological systems could alter NPs behavior. To tackle this issue, cell culture media are widely used as models resembling biological systems (25-27).

Typical culture media are buffered solutions containing serum proteins such as albumin and globulins along with amino acids and essential metal ions. Ionic strength is proved to be directly involve with degree of agglomeration of NPs (28). From the results, both SPION and SPION-CA tended to be aggregate when exposed to culture media. For uncoated SPION, with the surface containing O-H groups resulting from oxidation processes (29), electrostatic screening of the reactive hydroxyl groups with metal ions could occur, thus, lead to stability disruption (30). Coating of citrate molecules provided electrostatic repulsion to the SPIONs and greatly stabilized the NPs in water. However, when exposed to high ionic strength of culture media, the NPs formed aggregates resulting in size >1 μ m. These phenomena agree with the previous research where divalent ions such as Ca²⁺ and Mg²⁺ present in biological systems are able to form complexes with citrate ligands and destabilize the surface (31). Unlike small molecules, PMAA provides electronic repulsion with extra steric hindrance to prevent electronic screening and divalent metal ions chelation. Therefore, resulting in greater degree of stabilization in cell culture media with largest size of 500 nm in DMEM and increased to ~1.4 μ m when left for 24 hours (figure 3b).

Beside surface modification, serum proteins were reported to be non-trivial to NPs behavior (32, 33) and, when used at proper concentration, could promote colloidal stability (31, 34). In this research, FBS was found to stabilize all SPION samples in biological media as observed from sizes reduction (figure 3d and 3f). Albumin proteins presenting in FBS are known to attach on NPs surface,

forming protein coronas. With corona formation, NPs surface is protected and contacting with ions is prevented, thus, reducing interference from the electrolytes.

The importance of stabilization of the NPs in biological uses is demonstrated in cellular uptake experiments with MCF-7 breast cancer cells. SPION-PMAA, exhibiting highest colloidal stability, showed clear cellular uptake with minimal non-specific attachment to the coverslip and cell surface. The non-stable uncoated SPIONs formed large aggregates, therefore, cellular uptake could not be clearly observed. Surprisingly, SPION-CA showed the highest cellular uptake despite larger hydrodynamic diameter when compared to SPION-PMAA. These results could be due to the steric hindrance of PMAA showing adverse effects on cellular uptake behavior or different in surface charge distribution and concentration as previously reported that negatively-charged NPs tend to be uptake more into the cells (10, 11).

Conclusion

In conclusion, we have demonstrated the effect of serum proteins on the stability, cytotoxicity and cellular uptake activities of SPION, SPION-PMAA and SPION-CA. As destabilizing effects of biological environment originated dominantly from ions complexation. Modification of the NPs surface to prevent direct electrostatic interaction through steric hindrance is one method to stabilize the NPs. The presence of serum proteins in the environment could also enhance the stability of the NPs by formation of protein coronas with additional effect on reducing the cytotoxicity toward MCF-7 breast cancer cells. However, for biomedical applications, balancing between steric and electronic properties is essential for utilization of NPs as demonstrated with higher uptake level of SPION-CA. Therefore, this research emphasizes the importance of NPs behavior in relevant biological environmental conditions which is important for development and improvement of safe and effective targeting NPs for cancer therapeutic or diagnostic applications.

Acknowledgments

This project was supported by Mahidol University and the Faculty of Science, Mahidol University, and the Thailand Research Fund (IRG5980008, RTA5980001, MRG5980041). WM was supported by a Science Achievement Scholarship of Thailand. This project was partially supported by a CIF grant, Center of Nanoimaging and DKSH center of excellence, Faculty of Science, Mahidol University.

Conflicts of interest

References

- 1. Tietze R, Zaloga J, Unterweger H, Lyer S, Friedrich RP, Janko C, et al. Magnetic nanoparticle-based drug delivery for cancer therapy. Biochem Biophys Res Commun. 2015;468(3):463-70.
- 2. Knezevic NZ, Lin VSY. A magnetic mesoporous silica nanoparticle-based drug delivery system for photosensitive cooperative treatment of cancer with a mesopore-capping agent and mesopore-loaded drug. Nanoscale. 2013;5(4):1544-51.
- 3. Maham M, Karami-Osboo R. Extraction of sulfathiazole from urine samples using biosynthesized magnetic nanoparticles. Iran J Pharm Res. 2017;16(2):462-70.
- 4. Ho D, Sun X, Sun S. Monodisperse magnetic nanoparticles for theranostic applications. Acc Chem Res. 2011;44(10):875-82.
- 5. Mahmed N, Heczko O, Lancok A, Hannula SP. The magnetic and oxidation behavior of bare and silica-coated iron oxide nanoparticles synthesized by reverse co-precipitation of ferrous ion (Fe²⁺) in ambient atmosphere. J Magn Magn Mater. 2014;353(Supplement C):15-22.
- 6. Kotsmar C, Yoon KY, Yu H, Ryoo SY, Barth J, Shao S, et al. Stable citrate-coated iron oxide superparamagnetic nanoclusters at high salinity. Ind Eng Chem Res. 2010;49(24):12435-43.
- 7. He YP, Wang SQ, Li CR, Miao YM, Wu ZY, Zou BS. Synthesis and characterization of functionalized silica-coated Fe₃O₄ superparamagnetic nanocrystals for biological applications. J Phys D Appl Phys. 2005;38(9):1342.
- 8. Mancarella S, Greco V, Baldassarre F, Vergara D, Maffia M, Leporatti S. Polymer-coated magnetic nanoparticles for curcumin delivery to cancer cells. Macromol Biosci. 2015;15(10):1365-74.
- 9. Laurent S, Saei AA, Behzadi S, Panahifar A, Mahmoudi M. Superparamagnetic iron oxide nanoparticles for delivery of therapeutic agents: opportunities and challenges. Expert Opin Drug Deliv. 2014;11(9):1449-70.
- 10. Fröhlich E. The role of surface charge in cellular uptake and cytotoxicity of medical nanoparticles. Int J Nanomedicine. 2012;7:5577-91.
- 11. King Heiden TC, Dengler E, Kao WJ, Heideman W, Peterson RE. Developmental toxicity of low generation PAMAM dendrimers in zebrafish. Toxicol Appl Pharmacol. 2007;225(1):70-9.
- 12. Tural B, Kaya M, Özkan N, Volkan M. Preparation and characterization of Ni-nitrilotriacetic acid bearing poly(methacrylic acid) coated superparamagnetic magnetite nanoparticles. J Nanosci Nanotechno. 2008;8(2):695-701.
- 13. Pino Pd, Pelaz B, Zhang Q, Maffre P, Nienhaus GU, Parak WJ. Protein corona formation around nanoparticles from the past to the future. Mater Horiz. 2014;1(3):301-13.
- 14. Halamoda-Kenzaoui B, Ceridono M, Colpo P, Valsesia A, Urbán P, Ojea-Jiménez I, et al. Dispersion behaviour of silica nanoparticles in biological media and its influence on cellular uptake. PLoS One. 2015;10(10):e0141593.
- 15. Wiogo HTR, Lim M, Bulmus V, Yun J, Amal R. Stabilization of magnetic iron oxide nanoparticles in biological media by fetal bovine serum (FBS). Langmuir. 2011;27(2):843-50.
- 16. Yan Y, Gause KT, Kamphuis MMJ, Ang C-S, O'Brien-Simpson NM, Lenzo JC, et al. Differential roles of the protein corona in the cellular uptake of nanoporous polymer particles by monocyte and macrophage cell lines. ACS Nano. 2013;7(12):10960-70.
- 17. Prapainop K, Wentworth P. A shotgun proteomic study of the protein corona associated with cholesterol and atheronal-B surface-modified quantum dots. Eur J Pharm Biopharm. 2011;77(3):353-9.
- 18. Prapainop K, Witter DP, Wentworth P. A chemical approach for cell-specific targeting of nanomaterials: small-molecule-initiated misfolding of nanoparticle corona proteins. J Am Chem Soc. 2012;134(9):4100-3.
- 19. Petcharoen K, Sirivat A. Synthesis and characterization of magnetite nanoparticles via the chemical co-precipitation method. Mater Sci Eng B-Adv. 2012;177(5):421-7.

- 20. Yu S, Chow GM. Carboxyl group (-CO2H) functionalized ferrimagnetic iron oxide nanoparticles for potential bio-applications. J Mater Chem. 2004;14(18):2781-6.
- 21. Nigam S, Barick KC, Bahadur D. Development of citrate-stabilized Fe₃O₄ nanoparticles: conjugation and release of doxorubicin for therapeutic applications. J Magn Magn Mater. 2011;323(2):237-43.
- 22. Mingwu S, Hongdong C, Xifu W, Xueyan C, Kangan L, Su He W, et al. Facile one-pot preparation, surface functionalization, and toxicity assay of APTS-coated iron oxide nanoparticles. Nanotechnology. 2012;23(10):105601.
- 23. Sperling RA, Parak WJ. Surface modification, functionalization and bioconjugation of colloidal inorganic nanoparticles. Philos T R Soc A. 2010;368(1915):1333-83.
- 24. Santra S, Tapec R, Theodoropoulou N, Dobson J, Hebard A, Tan WH. Synthesis and characterization of silica-coated iron oxide nanoparticles in microemulsion: The effect of nonionic surfactants. Langmuir. 2001;17(10):2900-6.
- 25. Ji Z, Jin X, George S, Xia T, Meng H, Wang X, et al. Dispersion and stability optimization of TiO2 nanoparticles in cell culture media. Environ Sci Technol. 2010;44(19):7309-14.
- 26. Sabuncu AC, Grubbs J, Qian S, Abdel-Fattah TM, Stacey MW, Beskok A. Probing nanoparticle interactions in cell culture media. Colloid Surface B. 2012;95:96-102.
- 27. Mahl D, Greulich C, Meyer-Zaika W, Koller M, Epple M. Gold nanoparticles: dispersibility in biological media and cell-biological effect. J Mater Chem. 2010;20(29):6176-81.
- 28. French RA, Jacobson AR, Kim B, Isley SL, Penn RL, Baveye PC. Influence of ionic strength, pH, and cation valence on aggregation kinetics of titanium dioxide nanoparticles. Environ Sci Technol. 2009;43(5):1354-9.
- 29. Wu W, He Q, Jiang C. Magnetic iron oxide nanoparticles: synthesis and surface functionalization strategies. Nanoscale Res Lett. 2008;3(11):397-415.
- 30. Allen LH, Matijević E. Stability of colloidal silica: I. effect of simple electrolytes. J Colloid Interf Sci. 1969;31(3):287-96.
- 31. Safi M, Courtois J, Seigneuret M, Conjeaud H, Berret JF. The effects of aggregation and protein corona on the cellular internalization of iron oxide nanoparticles. Biomaterials. 2011;32(35):9353-63.
- 32. Lesniak A, Fenaroli F, Monopoli MP, Aberg C, Dawson KA, Salvati A. Effects of the presence or absence of a protein corona on silica nanoparticle uptake and impact on cells. ACS Nano. 2012;6(7):5845-57.
- 33. Cedervall T, Lynch I, Lindman S, Berggard T, Thulin E, Nilsson H, et al. Understanding the nanoparticle-protein corona using methods to quantify exchange rates and affinities of proteins for nanoparticles. PNAS. 2007;104(7):2050-5.
- 34. Izak-Nau E, Voetz M, Eiden S, Duschl A, Puntes VF. Altered characteristics of silica nanoparticles in bovine and human serum: the importance of nanomaterial characterization prior to its toxicological evaluation. Part Fibre Toxicol. 2013;10(1):56.

American Association of Pharmaceutical Scientists Transfer of Copyright Agreement

konlova pra @mahidal adu				
Mahidol University, RamaVI Road, Bangkok, Thailand, Department of Biochemistry, School of Materials Science and Innovation, Faculty of Science, Mahidol University	_			
Corresponding Author's name, address, affiliation and email: Kanlaya Prapainop, Department of Biochemistry, Faculty of Science,	, Department of Biochemistry, Faculty of Science,			
(, (,				
Author(s) name(s): Wid Mekseriwattana, Supreeya Srisuk, Ruttanaporn Kriangsaksri, Nuttawee Niamsiri, Kanlaya Prapainop				
colloidal stability and cellular untake in breast cancer cells				
Title: The impact of serum proteins and surface chemistry on magnetic panoparticle	_			
Journal: 🔲 The AAPS Journal or 🔳 AAPS PharmSciTech				

The transfer of copyright gives AAPS the right to develop, promote, distribute, sell, and archive a body of scientific works in the United States and throughout the world (for government employees: to the extent transferable). The Author hereby grants and assigns to AAPS all rights in and to Author's work in and contributions to the Work. In connection with this assignment, the Author acknowledges that AAPS will have the right to print, publish, create derivative works, and sell the Work throughout the world, all rights in and to all revisions or versions or subsequent editions of the Work in all languages and media throughout the world, and shall be the sole owner of the copyright in the Work throughout the world. AAPS shall register the Work with the Copyright Office of the United States in its own name within four months after first publication.

If the Author is an employee of the U.S. Government and performed this work as part of their employment, the contribution is not subject to U.S. copyright protection. If the work was performed under Government contract, but the Author is not a Government employee, AAPS grants the U.S. Government royalty-free permission to reproduce all or part of the contribution and to authorize others to do so for U.S. Government purposes. If any of the above Authors on this agreement is an officer or employee of the U.S. Government reference will be made to this status in the signature.

An author may self-archive his/her accepted manuscript on his/her personal website provided that acknowledgement is given to the AAPS publication and a link to the published article on the journal website is inserted. An author may also deposit the accepted manuscript in a repository 12 months after publication in the journal, provided that acknowledgement is given to the AAPS publication and a link to the published article on the journal website is inserted. The Author must ensure that the publication by AAPS is properly credited and that the relevant copyright notice is repeated verbatim.

The Author reserves the following rights: (a) All proprietary rights other than copyrights, such as patent rights, (b) The right to use all or part of this article, including tables and figures in future works of their own, provided that the proper acknowledgment is made to the Publisher as copyright holder, and (c) The right to make copies of this article for his/her own use, but not for sale.

I warrant and represent that the Work does not violate any proprietary or personal rights of others (including, without limitation, any copyrights or privacy rights); that the Work is factually accurate and contains no matter libelous or otherwise unlawful; that I have substanxtially participated in the creation of the Work and that it represents my original work sufficient for me to claim authorship. I further warrant and represent that I have no financial interest in the subject matter of the Work or any affiliation with an organization or entity with a financial interest in the subject matter of the Work, other than as previously disclosed to the Association.

I have the consent of each author to transfer and assign any and all right, title, and interest; including copyright of the article referenced above. I hereby assign and transfer to the American Association of Pharmaceutical Scientists copyright and all rights under it. I further confirm that this article has not been published elsewhere, nor is it under consideration by any other publisher.

For applicable go	vernment employees only:	
		(Author Name), an Author on this paper, is an employee of and, by law, is not allowed to assign copyright. As corresponding
author, I therefore	consent below to have this	s article published without transfer of copyright.
Signature:	els: Trugu	Date: 26 october 2018
After completion	of this form please either t	mail the original signed form to the AAPS Editorial Office at the address

After completion of this form, please either mail the original signed form to the AAPS Editorial Office at the address below; fax the signed form to AAPS at +1.703.243.9532; or include the signed form in your manuscript submission.